Polymers **2015**, *7*, 418-452; doi:10.3390/polym7030418

OPEN ACCESS

polymers

ISSN 2073-4360

www.mdpi.com/journal/polymers

Article

Facile Synthesis of Well-Defined MDMO-PPV Containing (Tri)Block—Copolymers via Controlled Radical Polymerization and CuAAC Conjugation

Neomy Zaquen [1], Joke Vandenbergh [1], Maria Schneider-Baumann [2], Laurence Lutsen [3], Dirk Vanderzande [1,3] and Thomas Junkers [1,3,*]

[1] Polymer Reaction Design (PRD) Group, Instituut voor Materiaalonderzoek (IMO), Hasselt University, Agoralaan Building D, Diepenbeek B-3590, Belgium; E-Mails: neomy.zaquen@uhasselt.be (N.Z.); joke.vandenbergh@uhasselt.be (J.V.); dirk.vanderzande@uhasselt.be (D.V.)

[2] Institute for Polymer Chemistry and Chemical Technology, Preparative Macromolecular Chemistry, Karlsruhe Institute of Technology, Engesser str. 18, Karlsruhe 76128, Germany; E-Mail: maria.schneider@kit.edu

[3] IMEC associated laboratory IMOMEC, Wetenschapspark 1, Diepenbeek B-3590, Belgium; E-Mail: laurence.lutsen@uhasselt.be

* Author to whom correspondence should be addressed; E-Mail: thomas.junkers@uhasselt.be; Tel.: +32-1126-8318; Fax: +32-1126-8299.

Academic Editor: Alexander Böker

Received: 18 January 2015 / Accepted: 12 February 2015 / Published: 24 February 2015

Abstract: A systematic investigation into the chain transfer polymerization of the so-called radical precursor polymerization of poly(*p*-phenylene vinylene) (PPV) materials is presented. Polymerizations are characterized by systematic variation of chain transfer agent (CTA) concentration and reaction temperature. For the chain transfer constant, a negative activation energy of −12.8 kJ·mol^{-1} was deduced. Good control over molecular weight is achieved for both the sulfinyl and the dithiocarbamate route (DTC). PPVs with molecular weights ranging from thousands to ten thousands g·mol^{-1} were obtained. To allow for a meaningful analysis of the CTA influence, Mark–Houwink–Kuhn–Sakurada (MHKS) parameters were determined for conjugated MDMO-PPV ([2-methoxy-5-(3',7'-dimethyloctyloxy)]-1,4-phenylenevinylene) to $\alpha = 0.809$ and $k = 0.00002$ mL·g^{-1}. Further, high-endgroup fidelity of the CBr_4-derived PPVs was proven via chain extension experiments. MDMO-PPV-Br was successfully used as macroinitiator in atom transfer radical polymerization (ATRP) with acrylates and styrene.

A more polar PPV counterpart was chain extended by an acrylate in single-electron transfer living radical polymerization (SET-LRP). In a last step, copper-catalyzed azide alkyne cycloaddition (CuAAC) was used to synthesize block copolymer structures. Direct azidation followed by macromolecular conjugation showed only partial success, while the successive chain extension via ATRP followed by CuAAC afforded triblock copolymers of the poly(*p*-phenylene vinylene)-*block*-poly(*tert*-butyl acrylate)-*block*-poly(ethylene glycol) (PPV-*b*-P*t*BuA-*b*-PEG).

Keywords: poly(*p*-phenylene vinylene); MDMO-PPV; radical polymerization; chain transfer polymerization; (tri)block copolymers; ATRP; CuAAC

1. Introduction

Poly(*p*-phenylene vinylene)s (PPV)s are an important class of semiconducting polymer materials that display excellent optical and electrical properties and are one of the most studied conjugated polymers to date [1–4]. Throughout their history, PPVs have been used in a large variety of advanced applications, ranging from organic photovoltaic cells (OPVs), light emitting diodes (LEDs), field effect transistors (FET)s and biosensors [5,6]. Although other well-suited materials have made their way into the field of such electronic devices, PPVs are still interesting because of their high synthetic reliability and simple scale up possibilities [7], resulting in the potential high industrial relevance of these polymers [8,9]. Additionally, their outstanding fluorescence properties leave room for use in biomedical applications such as biosensors and fluorescent markers. Especially the latter has high potential for future endeavors. In order to target such applications, controlled polymerization methodologies need to be developed to reach a precision polymer design of these materials and to make them available for combination with other types of materials. Significant research has been performed towards the synthesis of PPVs, resulting in the indirect or so-called "precursor" route as the most established and reliable synthetic pathway [10–21]. The general polymerization mechanism proceeds via a self-initiating *p*-quinodimethane moiety, which is formed upon the 1,6-base elimination of a premonomer that then spontaneously polymerizes to form a precursor polymer [16,22,23]. Consequently, high conversions are easily reached within seconds to a few minutes enabling very fast polymerizations [24–27]. In a second step, elimination of the side group takes place, resulting in the desired conjugated polymer [15,23]. Over the last decades, different precursor routes were developed, for which the most important ones are the Gilch [11], Wessling [10,12,13], Xanthate [14,15], Sulfinyl [16–20] and Dithiocarbamate (DTC) route [28,29]. The sulfinyl route differs from the other routes since it is the only route in which an unsymmetrical premonomer is used and in which active monomer formation and prepolymer elimination can be fully separated from each other. Consequently, a better control over the polymerization is gained. Low defect levels in the polymer chain are obtained, enabling only head-tail couplings of the polymer chains, leading to soluble and high molecular weight polymers [16–21]. Depending on the base and the type of solvent used, sulfinyl polymerizations can either follow a controlled anionic pathway (lithium hexamethyldisilazide (LHMDS) as base and THF as solvent) [26,30] or a radical pathway (sodium *tert*-butoxide (Na*t*BuO) as base and *s*-BuOH as solvent) [31]. Recently, we have demonstrated how the optimized anionic pathway could be used for the synthesis of

amphiphilic fluorescent block copolymers [32–34], poly(*p*-phenylene vinylene)-*block*-poly(*tert*-butyl acrylate) (PPV-*b*-P*t*BuA) and poly(*p*-phenylene vinylene)-*block*-poly(ethylene glycol) (PPV-*b*-PEG) [35]. Anionic sulfinyl precursor polymerization is a highly promising technique, yet polymerizations must be carried out under very pure conditions and the selection of monomers is limited since not all derivatives can be polymerized in a purely anionic way. Thus, further evaluation and optimization of the radical polymerization route to likewise generate complex PPV-containing precision macromolecular materials is required.

Controlling radical PPV polymerizations is not as straightforward as in standard vinyl radical polymerizations because of the *in situ* formation of the *p*-quinodimethane system and its enormous driving force to propagate, which hinders interaction in any control equilibrium of a reversible deactivation radical polymerization (RDRP) [24–27]. During propagation (associated with the kinetic rate coefficient for propagation, k_p), aromaticity of the monomer is restored (see Scheme 1), resulting inevitably in a competition between the propagating radicals and the control agent. Nevertheless, previous studies towards radical PPV polymerizations have shown that the use of an excess of CBr_4 [36–39] as chain transfer agent (CTA) in combination with [2-methoxy-5-(3',7'-dimethyloctyloxy)]-1,4-phenylenevinylene (MDMO-PPV) as premonomer results in a successful molecular weight control in the polymerization and end group control of the polymers. Chain transfer polymerizations are inherently non-living, yet feature comparable control over product structures when carried out carefully (with the exception of product dispersity). A good correlation between the inverse of the molecular weight of the conjugated PPVs and the CTA concentration was obtained, following the expected Mayo behavior. Number average molecular weights (M_n) ranging from 12,000 to 25,000 g·mol^{-1} were obtained in an initial study, compared to M_n values of over 100,000 g·mol^{-1} for PPVs synthesized typically via the uncontrolled radical pathway. The transfer constant C_{tr} of CBr_4 was determined to be ~0.003. Despite this very low value, still good and reproducible control was achieved when several equiv. of chain transfer agents are used. By transfer reactions, the resulting precursor MDMO–PPV contains bromine end-group functionalities which can be reactivated in a next step using atom transfer radical polymerization (ATRP) conditions [40,41]. The proof of principle for block copolymer synthesis including precursor PPVs was demonstrated using styrene as monomer and Cu(I)Br/*N*,*N*,*N*′,*N*′,*N*″-pentamethyldiethylenetriamine (PMDETA) as metal/ligand system, thereby proving that chain extension of bromine-functionalized PPVs were in principle possible using copper-mediated polymerization [39]. However, further data is required to fully understand the involved limitations and underpinning challenges since only very preliminary data was provided.

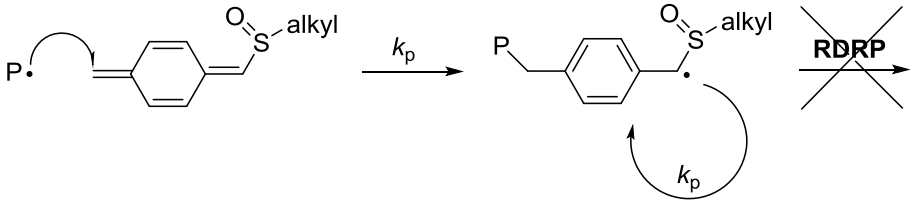

Scheme 1. Propagation reaction in precursor polymerization. Aromaticity is restored during propagation, which renders reversible deactivation radical polymerization (RDRP) inaccessible.

In here, we thus focus in-depth on two different aspects of the polymerization method described above. First, we discuss in detail the kinetics of the process on the basis of a broad dataset generated for CBr_4-controlled precursor polymerization. Subsequently, we explore the synthetic potential of the technique compared to our previous study. For the kinetic study, we focus on the controlled synthesis of MDMO-PPV and 6-(2-chloromethyl-4-methoxy-5-[(octylsulfinyl)methyl]-phenoxy) hexanioc-acid methyl ester (CPM-PPV) using CBr_4 as CTA. Also, differences between the sulfinyl and the dithiocarbamate (DTC) precursor route are elucidated. The range of polymer chain lengths that is accessible is thoroughly determined and activation energies for the transfer constant are derived shining light on the not yet fully resolved precursor polymerization mechanism. Secondly, the scope of the ATRP chain extension of sulfinyl precursor MDMO-PPV is extended by synthesizing a variety of block copolymers with styrene or *t*-butyl acrylate to obtain well-defined PPV-*b*-PS and PPV-*b*-P*t*BuA with varying block lengths and compositions. Finally, end group modification and subsequent conjugation of the PPV-*b*-P*t*BuA block copolymers using copper catalyzed azide-alkyne cycloaddition (CuAAC) click-chemistry results in an (comparatively) easy to purify PPV-*b*-P*t*BuA-*b*-PEG triblock copolymer—the first of their kind to the best of our knowledge. By combining the excellent optoelectronic properties of PPVs with the advantages of CRP routes, a new generation of highly specific precision block copolymer materials with advanced architecture and sophisticated physical properties becomes available, opening new avenues for conjugated materials outside the field of organic electronics [42,43].

2. Experimental Section

2.1. Materials

All materials and reagents were purchased from Acros or Sigma Aldrich and were used without further purification. Tetrahydrofurane (THF), dimethylformamide (DMF) and CH_2Cl_2 were dried on a MB-SPS 800 system (MBraun, Garching, Germany). *tert*-Butyl acrylate and styrene were deinhibited over a column of basic alumina.

2.2. Analysis

^{1}H-NMR spectra were recorded in $CDCl_3$ on a Varian Inova 300 spectrometer (Varian: Palo Alto, CA, USA) at 300 and 75 MHz, respectively, using a 5 mm probe. FT-IR (Fourier transform infrared spectoscopy) spectra were collected on a Brucker Tensor 27 spectrophotometer (Brucker: Brussels, Belgium) (nominal resolution 4 cm^{-1}). Direct insertion probe/mass spectrometry (DIP MS) analyses were obtained with a Varian TSQ-70 and a Voyager mass spectrometer (Thermoquest, Waltham, CA, USA). The capillary column was a Chrompack Cpsil5CB or Cpsil8CB. Analytical SEC (Size Exclusion Chromatography) was performed on a Tosoh EcoSEC (Tosoh, Stuttgart, Germany) HLC-8320GPC, comprising an autosampler, a Polymer Standard Service (PSS) guard column Styrene Divinyl Benzene (SDV) (50 × 7.5 mm), followed by three PSS SDV analytical linear XL (5 µm, 300 × 7.5 mm) columns thermostatted at 40 °C (column molecular weight range: 1×10^2–1×10^6 g·mol^{-1}), and a differential refractive index detector (Tosoh EcoSEC RI) using THF as the eluent at a flow rate of 1 mL·min^{-1}. Toluene was used as a flow marker. Calibration was performed using linear narrow polystyrene (PS) standards from PSS Laboratories in the range of 470−7.5×10^6 g·mol^{-1}. Although

correct Mark Houwink parameters for plain precursor ($\alpha = 0.67605$ and $k = 0.000142$ mL·g^{-1}) as well as conjugated MDMO–PPV ($\alpha = 0.809$ and $k = 0.00002$ mL·g^{-1}) were used, differences in these parameters upon the formation of (tri) block copolymers were not taken into account. Therefore, only apparent values for (tri)block copolymers are discussed. Analysis of the molecular weight distributions (MWD)s of the polymers with UV detection at λ_{max} of the polymer was performed using a Spectra Series P100 (Spectra Physics, Santa Clara, CA, USA) pump equipped with two mixed-B columns (10 µm, 2 cm × 30 cm, Polymer Laboratories (Varian, Palo Alto, CA, USA) and an Agilent 1100 Diode Array Detector (DAD) UV detector at 60 °C. Chlorobenzene (CB) was used as the eluent at a flow rate of 1.0 mL·min^{-1}. Molecular weights were determined relative to polystyrene standards. UV-Vis spectra were recorded on a Varian Cary 500 UV-Vis-NIR spectrophotometer (scan rate 600 nm·min^{-1}, continuous run from 200 to 800 nm). Separation of polymers after selective precipitation were performed on a recycling preparative HPLC (JAI, Zutphen, The Netherlands) (high performance liquid chromatography) LC-9210 NEXT system in the recycle injection mode (3 mL) comprising a JAIGEL-2H and JAIGEL-3H column and a NEXT series UV detector using $CHCl_3$ as the eluent with a flow rate of 3.5 mL·min^{-1}.

2.3. Determination of Mark–Houwink Parameters

MHKS parameters are determined by measuring the intrinsic viscosity ([η]) of several MDMO-PPV distributions of known molecular weight [M_w] (determined using an independent method, e.g., Multi Angle Laser Light Scattering (MALLS)). Via usage of these polymer samples with precisely known mass, d*n*/d*c* is directly obtained from the Refractive Index (RI) detector signal and MHKS values can be fitted from the light scattering M_w data. For sulfinyl MDMO precursor polymer $\alpha = 0.67605$ and $k = 0.000142$ mL·g^{-1} and for conjugated MDMO-PPV $\alpha = 0.809$ and $k = 0.00002$ mL·g^{-1} was obtained.

2.4. Monomer Synthesis

Synthesis of 1-(chloromethyl)-5-((3,7-dimethyloctyl)oxy)-2-methoxy-4-((octylsulfinyl)methyl) benzene (MDMO-sulfinyl) premonomer, 6-(5-chloromethyl-4-methoxy-2-octylsulfinylmethylphenoxy)hexanoic acid methyl ester (CPM) sulfinyl premonomer and 2,5-bis(*N*,*N*-diethyldithiocarbamate-methyl)-1-(3,7-dimethyloctyloxy)-4-methoxybenzene (MDMO-DTC) premonomer are described in Appendix Schemes A1–A3.

2.5. Polymerization

2.5.1. General Method for the Polymerization of Bromine-Functionalized MDMO (P1) or CPM (P2) Sulfinyl Precursor PPV

A solution of MDMO sulfinyl premonomer **7** (1.00 g, 2.05 mmol, 1 equiv.) and CBr_4 (5.44 g, 16.4 mmol, 8 equiv.) in *s*-butanol (14.8 mL) and a solution of Na*t*BuO (0.256 g, 2.67 mmol, 1.3 equiv.) in *s*-butanol (16.8 mL) were degassed three times at 30 °C using nitrogen. The base solution was added in one portion to the stirred monomer solution to start the reaction. After 1 h, the reaction was quenched with HCl (1 M, 50.0 mL). After extraction with CH_2Cl_2 (3 mL × 50 mL) and evaporation, the product was dissolved in $CHCl_3$ (15 mL) and precipitated in cold methanol (100 mL). The mixture was

filtered on a Teflon® filter and the polymer was collected and dried *in vacuo*. The crude product was purified via preparative recycling SEC to yield the pure polymer **P1** as a yellow viscous oil (72%), Scheme 2. SEC (THF): M_n^{app} = 10,100 g·mol^{-1}, $Đ$ = 1.9. ^{1}H-NMR ($CDCl_3$): δ = 6.90–6.20 (m, 2H); 4.90–4.60 (t, 1H); 4.00–2.90 (m, 7H); 2.70–2.10 (t, 2H); 1.90–1.10 (m, 22H); 1.00–0.80 (m, 12H). ^{13}C-NMR ($CDCl_3$): δ = 151.40 (C4); 127.0 (C4); 110.50 (CH); 67.90 (CH_2); 59.10–55.10 (CH); 56.40 (CH_3); 49.70 (CH_2); 39.20 (CH_2); 37.40 (CH_2); 36.60 (CH_2); 32.10–29.10 (CH_2); 30.20 (CH_2); 27.90 (CH_2); 24.60 (CH_2); 22.60 (CH_2); 21.90 (CH_3); 19.80 (CH_3); 13.50 (CH_3). FT-IR (NaCl): 2955, 2927, 1509, 1471, 1462, 1413, 1222, 1031 cm^{-1}.

Synthesis of bromine-functionalized CPM sulfinyl precursor PPV **P2** was similar to synthesize the MDMO precursor PPV, Scheme 2. SEC (THF): M_n^{app} = 9800 g·mol^{-1}, $Đ$ = 1.8. ^{1}H-NMR ($CDCl_3$): δ = 7.00–6.20 (m, 2H); 4.50 (m, 2H); 4.10–3.60 (m, 6H); 3.40 (m, 2H); 2.40–1.80 (t, 4H); 1.80–1.20 (m, 18H); 0.90 (m, 3H). ^{13}C-NMR ($CDCl_3$): δ = 173.2 (C4); 151.20 (C4); 125.0 (C4); 114.50 (CH); 68.20 (CH_2); 61.0 (CH_2); 56.20 (CH_3); 51.90 (CH_3); 49.60 (CH_2); 33.20 (CH_2); 31.40 (CH_2); 29.10–22.80 (CH_2); 14.50 (CH_3). FT-IR (NaCl): 2929, 2856, 1728, 1506, 1463, 1409, 1212, 1032 cm^{-1}.

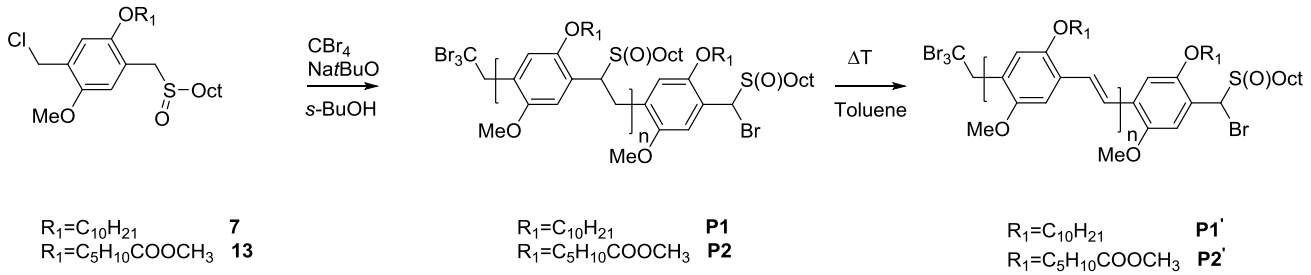

Scheme 2. Synthesis of MDMO-PPV and CPM-PPV via the sulfinyl precursor route using CBr_4 as CTA.

2.5.2. General Method for the Elimination of Bromine-Functionalized MDMO (P1') or CPM (P2') Sulfinyl PPV

Precursor PPV **P1** (200 mg) in toluene (15 mL) was degassed by purging for 15 min with nitrogen, after which the solution was heated to 110 °C and stirred for 3 h under nitrogen atmosphere. Subsequently, the reaction was cooled down to room temperature and precipitated in cold MeOH (40 mL) and filtered on a Teflon® filter. The conjugated MDMO–PPV polymer **P1'** was obtained as a red solid (75%), Scheme 2. SEC (THF): M_n^{app} = 11,500 g·mol^{-1}, $Đ$ = 1.7. ^{1}H-NMR ($CDCl_3$): δ = 7.49 (m, 2H); 7.19 (m, 2H); 4.60–3.20 (m, 5H); 2.10–0.6 (m, 19H). ^{13}C-NMR ($CDCl_3$): δ = 151.40 (C4); 127.0 (C4); 110.50 (CH); 108.85 (CH); 67.90 (CH_2); 56.40 (CH_3); 39.20 (CH_2); 37.40 (CH_2); 36.60 (CH_2); 30.20 (CH_2); 27.90 (CH_2); 24.60 (CH_2); 22.60 (CH_2); 19.80 (CH_3). FT-IR (KBr): 2957, 2925, 2860, 1510, 1469, 1395, 1217, 1028, 872 cm^{-1}.

Synthesis of bromine-functionalized conjugated CPM-PPV **P2'** was similar to synthesis of the MDMO-PPV, Scheme 2. SEC (THF): M_n^{app} = 11,800 g·mol^{-1}, $Đ$ = 1.6. ^{1}H-NMR ($CDCl_3$): δ = 7.50–7.3 (m, 2H); 7.20–6.90 (m, 2H); 4.20 (m, 2H); 3.8 (t, 3H); 3.6 (m, 2H); 2.30–0.6 (m, 6H). ^{13}C-NMR ($CDCl_3$): δ = 173.1 (C4); 153.30 (C4); 150.8 (C4); 127.2 (C4); 123.2, 110.40 (CH); 69.00 (CH_2); 56.10 (CH_3); 51.90 (CH_3); 49.60 (CH_2); 33.80 (CH_2); 28.60–24.70 (CH_2); 14.50 (CH_3). FT-IR (NaCl): 2934, 2866, 1728, 1505, 1205, 1034, 969 cm^{-1}.

2.5.3. General Method for the Polymerization of Bromine-Functionalized MDMO (P3) DTC Precursor PPV

A solution of premonomer **18** in THF (0.5 g, 0.851 mmol, 1 equiv.) and CBr_4 (0.0282 g, 0.0851 mmol, 0.1 equiv.) in THF (4.23 mL) and a solution of K*t*BuO (0.143 g, 1.28 mmol, 1.5 equiv.) in THF (1.47 mL) were degassed three times at 35 °C using nitrogen. The base solution was added in one portion to the stirred monomer solution to start the reaction. After 1.5 h, the reaction was quenched with HCl (1 M, 50.0 mL). After extraction with CH_2Cl_2 (3 × 50 mL) and evaporation, the product was dissolved in $CHCl_3$ (15 mL) and precipitated in cold methanol (100 mL) The mixture was filtered on a Teflon® filter and the polymer **P3** was collected and dried *in vacuo* resulting in a yellow viscous oil (72%), Scheme 3. SEC (THF): M_n^{app} = 11,900 g·mol^{-1}, $Đ$ = 2.3. ^{1}H NMR ($CDCl_3$): δ = 6.45–6.97 (m, 2H); 5.50–5.87 (s, 1H); 3.05–4.23 (m, 11H); 1.02–1.95 (m, 16H); 0.74–1.02 (m, 9H); ^{13}C NMR ($CDCl_3$): δ = 195.76 (C4); 150.85 (C4); 127.68 (C4); 114.11 (CH); 113.09 (CH); 67.10 (CH_2); 56.39 (CH_3); 51.98 (CH_2); 49.08 (CH_2); 46.38 (CH_2); 39.27 (CH_2); 37.54 (CH_2); 36.60 (CH_2); 34.45 (CH_2); 29.91 (CH_2); 27.92 (CH_2); 24.67 (CH_3); 22.69 (CH_3); 22.58(CH_3); 19.66 (CH_2); 12.47 (CH_3); 11.55 (CH_3). FT-IR (NaCl): 2953, 2929, 1504, 1484, 1462, 1413, 1267, 1210, 1140, 1041 cm^{-1}.

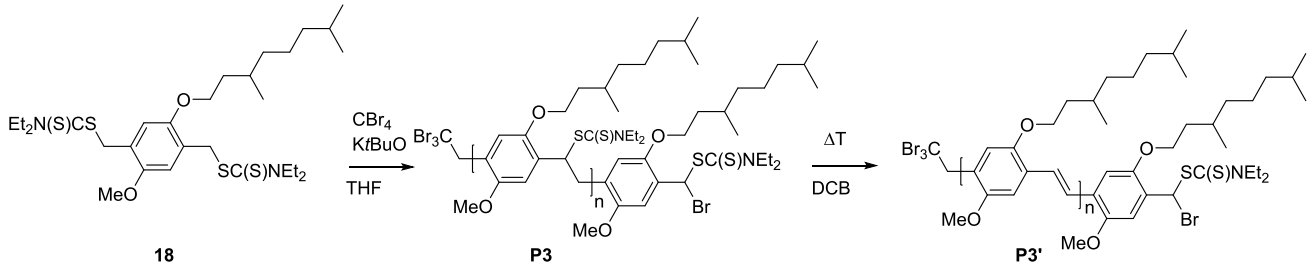

Scheme 3. Synthesis of MDMO-PPV via the DTC precursor route using CBr_4 as CTA.

2.5.4. General Method for the Elimination of Bromine-Functionalized MDMO (P3') DTC PPV

Precursor PPV **P3** (200 mg) in dichlorobenzene (60 mL) was degassed by purging for 15 min with nitrogen, after which the solution was heated to 180 °C and stirred for 3 h under nitrogen atmosphere. Subsequently, the reaction was cooled down to room temperature and precipitated in cold MeOH (40 mL) and filtered on a Teflon® filter. The conjugated MDMO-PPV polymer **P3'** was obtained as a red solid (75%), Scheme 3. SEC (THF): M_n^{app} = 15,300 g·mol^{-1}, $Đ$ = 1.8. ^{1}H NMR ($C_2D_2Cl_4$): δ = 7.50 (2H); 7.21 (2H); 4.61–3.19 (m, 5H); 2.10–0.59 (m; 19H). ^{13}C NMR ($CDCl_3$): δ = 151.4 (C4); 127.0 (C4); 123.3 (C4); 110.5 (CH); 108.8 (CH); 67.9 (CH_2); 56.4 (CH_3); 39.2 (CH_2); 37.4 (CH_2); 36.6 (CH_2); 30.2 (CH_2); 27.9 (CH_2); 24.6 (CH_3); 22.6 (CH_3); 19.8 (CH_3). FT-IR (KBr): 2957, 2925, 2860, 1510, 1469, 1395, 1217, 1028, 872 cm^{-1}.

2.6. Chain Extension of PPVs

2.6.1. Block Extension Using MDMO Sulfinyl Precursor PPV P1 as Macro Initiator

For the block copolymerization with *t*-butyl acrylate (*t*BuA), the precursor PPV **P1**—purified by recycling Gel Permeation Chromatography (GPC)—was used as macroinitator. A Schlenk tube was filled with Cu(I)Br (4.5 mg, 7.15 μmol, 1.1 equiv.), *t*BuA (75 mg, 0.580 mmol, 100 equiv.), Me_6tren (tris[2-

(dimethylamino)ethyl]amine, 14.3 μmol, 3.30 μL, 2.2 equiv.) and **P1** (M_n^{app} = 7700 g·mol^{-1}, 0.1 g, 5.8 μmol, 1 equiv.) dissolved in BuOAc (1 mL). The Schlenk tube was subjected to three freeze-pump-thaw cycles and transferred into the glovebox. The reaction mixture was stirred at 75 °C, and at specified times, samples were taken. The sample mixtures were poured in an aluminum tray and precipitated in a MeOH/H_2O (4/1) mixture. After evaporation of the solvent, the polymer was filtered over a small alumina column to remove all copper and the solvent was evaporated. A bright yellow viscous precursor MDMO-PPV-*b*-P*t*BuA **BP1** polymer was obtained after filtration, Scheme 4. SEC (THF): M_n^{app} = 8300–10,800 g·mol^{-1}, $Đ$ = 2.3.

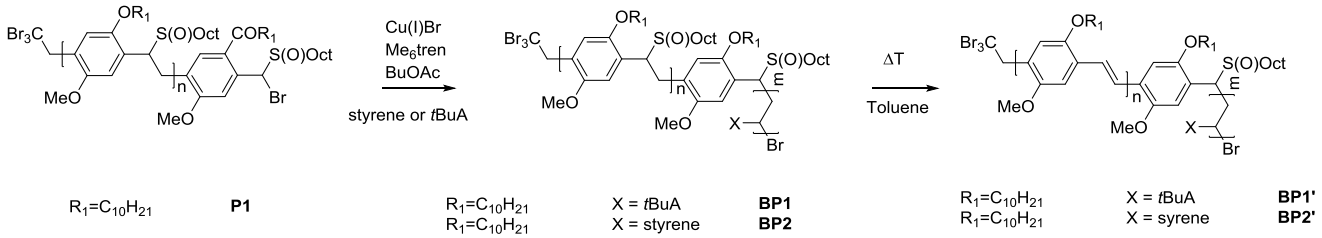

Scheme 4. Synthesis of MDMO-PPV-*b*-P*t*BuA and MDMO-PPV-*b*-PS block copolymers using ATRP chain extensions.

Block extensions on **P1** were varied in the type of monomer (styrene instead of *tert*-butyl acrylate) and in number of monomer equiv. (50 and/or 100). All chain extensions were performed using the synthesis procedure described above. However, precipitation of the precursor MDMO-PPV-*b*-PS **BP2** block copolymers was performed in MeOH.

2.6.2. Thermal Elimination of the Precursor MDMO-PPV-*b*-P*t*BuA BP1 and MDMO-PPV-*b*-PS BP2 Block Copolymers

Precursor MDMO-PPV-*b*-P*t*BuA block copolymer **BP1** (200 mg) in toluene (15 mL) was degassed by purging for 15 min with nitrogen, after which the solution was heated to 110 °C and stirred for 3 h under nitrogen atmosphere. Subsequently, the reaction was cooled down to room temperature and precipitated in cold MeOH/H_2O (4/1) mixture (40 mL) and filtered on a Teflon® filter. The conjugated polymer was obtained as a reddish oil **BP1'** (75%), Scheme 4. SEC (THF): M_n^{app} = 8300 g·mol^{-1}, $Đ$ = 2.10. A similar procedure was used for the thermal elimination of precursor MDMO-PPV-*b*-PS **BP2** into conjugated **BP2'** which also was obtained as a red solid (70%). SEC (THF): M_n^{app} = 15,300 g·mol^{-1}, $Đ$ = 1.9.

2.6.3. Synthesis of Azide-Functionalized Precursor MDMO-PPV-N_3 **Pn1**

To a stirred solution of **P1** (M_n^{app} = 9000 g·mol^{-1}, 0.1714 g, 1.9 μmol, 1 equiv.) in DMF (5 mL) sodium azide (12.9 mg, 19.0 μmol, 10 equiv.) was added. The mixture was stirred for 72 h at elevated temperature, after which cold water was added to the flask. The polymer was extracted with $CHCl_3$ (3 × 100 mL) and subsequent evaporation of the organic layer and precipitation in MeOH, resulted after filtration in the azide-functionalized precursor MDMO-PPV-N_3 **Pn1** (85%), Scheme 5.

2.6.4. Conjugation of Precursor MDMO-PPV-N_3 Pn1 Using CuAAC Click Conditions

To a solution of **Pn1** (M_n^{app} = 9000 g·mol^{-1}, 0.1 g, 16.7 µmol, 1 equiv.), **PEG-alkyne** [44] (1 equiv.) and Cu(I)Br (11.9 mg, 83.0 µmol, 5 equiv.) in dry DMF (5 mL), Me_6tren (19.1 mg, 83.0 µmol, 5 equiv.) was added under nitrogen atmosphere. The reaction mixture was stirred for 72 h at room temperature. The solution was passed through a neutral alumina column in order to remove the copper salts and concentrated under reduced pressure to obtain **Pc1** as an orange viscous oil (43%), Scheme 5. SEC (THF): M_p^{app} = 15,800 g·mol^{-1} $Đ$ = n.a.

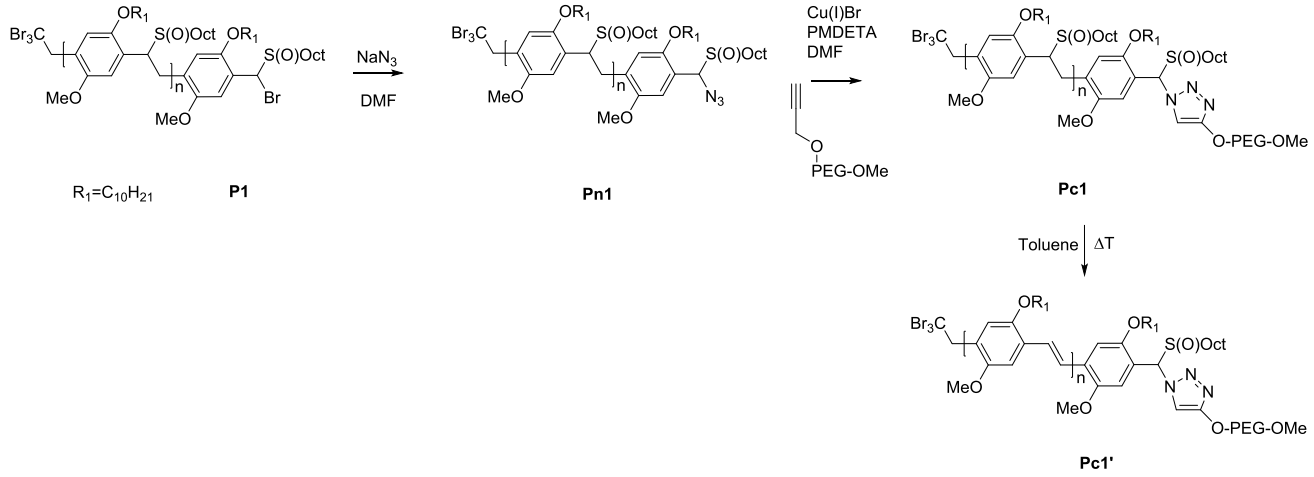

Scheme 5. Synthesis of PPV block copolymers using click conditions.

2.6.5. Thermal elimination of the precursor MDMO-PPV-*b*-PEG diblock copolymer into Pc1'

Precursor block copolymer **Pc1** (100 mg) in toluene (15 mL) was degassed by purging for 15 min with nitrogen, after which the solution was heated to 110 °C and stirred for 3 h under nitrogen atmosphere. Subsequently, the reaction was cooled down to room temperature and precipitated in ice cold MeOH, (40 mL) and filtered. The conjugated block-copolymer **Pc1'** was obtained as a red solid (75%), Scheme 5. SEC (THF): M_p^{app} = 18,400 g·mol^{-1}, $Đ$ = n.a.

2.6.6. Synthesis of Azide-Functionalized Precursor MDMO-PPV-*b*-P*t*BuA-N_3 BPn1

To a stirred solution of **BP1** (M_n^{app} = 6400 g·mol^{-1}, 0.1 g, 7.8 µmol, 1 equiv.) in DMF (5 mL) sodium azide (5.4 mg, 78.7 µmol, 10 equiv.) was added. The mixture was stirred for 72 h at room temperature, after which cold water was added to the flask. The polymer was extracted with $CHCl_3$ (3 × 100 mL) and subsequent evaporation of the organic layer and precipitation in a MEOH/H_2O (4/1) mixture resulted after filtration in the azide-functionalized precursor MDMO-PPV-*b*-P*t*BuA-N_3 **BPn1**, Scheme 6.

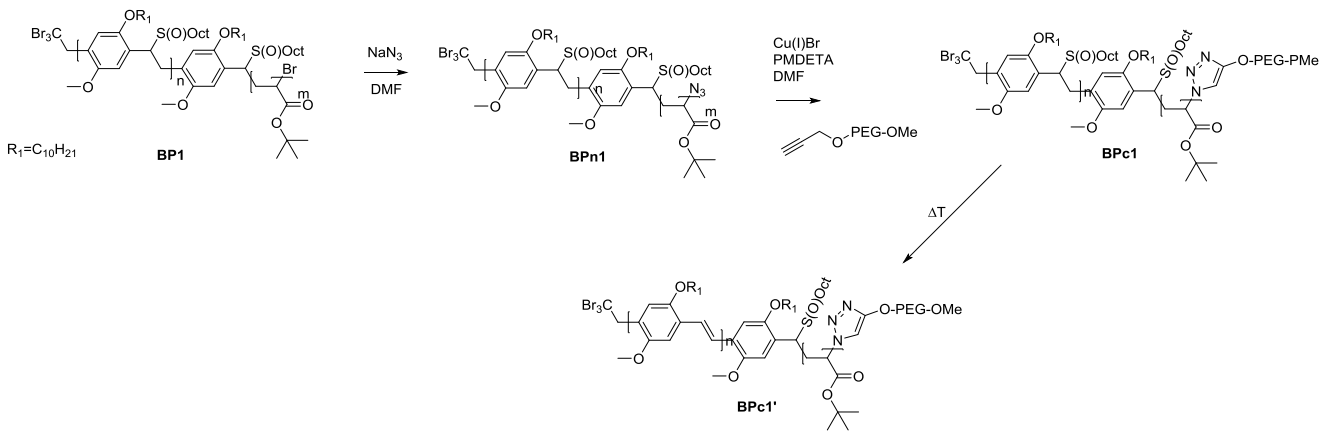

Scheme 6. Synthesis of PPV tri-block copolymers using click conditions.

2.6.7. Conjugation of Precursor MDMO-PPV-I-P*t*BuA-N_3 BPn1 Using CuAAC Click Conditions

To a solution of **BPn1** (M_n^{app} = 6300 g·mol^{-1}, 0.1 g, 13.7 µmol, 1 equiv.), **PEG-alkyne** [45] (1 equiv.) and Cu(I)Br (9.8 mg, 68.5 µmol, 5 equiv.) in dry DMF (5 mL), Me_6tren (15.8 mg, 68.5 µmol, 5 equiv.) was added under nitrogen atmosphere. The reaction mixture was stirred for 72 h at room temperature. The solution was passed through a neutral alumina column in order to remove the copper salts and concentrated under reduced pressure to obtain **BPc1** as an orange viscous oil (68%), Scheme 6. SEC (THF): M_n^{app} = 12,700 g·mol^{-1}, $Đ$ = 1.5.

2.6.8. Thermal Elimination of the Precursor MDMO-PPV-*b*-P*t*BuA-*b*-PEG Triblock Copolymer BPc1

Precursor block copolymer **BPc1** (200 mg) in toluene (15 mL) was degassed by purging for 15 min with nitrogen, after which the solution was heated to 110 °C and stirred for 3 h under nitrogen atmosphere. Subsequently, the reaction was cooled down to room temperature and precipitated in ice cold hexane (40 mL) and filtered. The conjugated triblock-copolymer **BPc1'** was obtained as a red polymer (75%), Scheme 6. SEC (THF): M_n^{app} = 13,400 g·mol^{-1}, $Đ$ = 1.4.

3. Results and Discussion

3.1. Control over the Radical PPV Polymerization by Using a CTA

A general pathway to gain control over radical polymerizations is to add control agents to the polymerization that involve the propagating radicals in reversible deactivation equilibria, leading to linear growth of chains with monomer conversion and general preselection of M_n of the final polymer depending on control agent concentration. As mentioned above, achieving such reversible deactivation is not as straightforward for PPV polymerizations as for conventional radical polymerizations. During initiation (formation of a biradical) as well as during propagation of the *p*-quinodimethane monomers, aromaticity is restored, resulting in a very high driving force for these reactions. Therefore, initiation and propagation are extremely fast and only those control agents that allow for similarly high reactivities will be able to compete. So far, no control agent from the typical RDRP methods could be identified to be effectively operational in precursor polymerizations. Only CBr_4—a classical chain transfer agent that induces molecular weight control, but not livingness of the polymerization—had been found to be active

enough to have a direct (and positive) influence on the polymer product. A good correlation between the molecular weight of conjugated MDMO-PPV—synthesized via the sulfinyl route—and the transfer agent concentration is reported in a previous study [39], resulting in polymers with molecular weights ranging from a M_n of 12,000 to 25,000 g·mol^{-1} with a dispersity ($Đ$) of ~2.0.

In this study, the effect of CBr_4 on the polymerization of PPV is compared between two precursor routes, e.g., the sulfinyl and the dithiocarbamate (DTC) route. Polymerizations via the sulfinyl route show very fast reactions reaching conversions of almost 100% in less than 5 min. As a result, the addition of high excesses of control agent is needed to obtain the desired effect. Polymerizations using the DTC route on the other hand result in slower polymerizations, and reactions only reach full conversion after 10–15 min. This indicates that good control over the DTC polymerization route using less control agent should be possible. Therefore, three different PPV premonomers were synthesized (see Scheme 7), namely the so-called MDMO sulfinyl premonomer, CPM sulfinyl premonomer and MDMO DTC premonomer. The two MDMO monomers lead equally to the formation of MDMO-PPV, a common conjugated material used in a multitude of applications. The CPM premonomer is used for the synthesis of a close derivative, which is interesting due to the possibility to post-functionalize the conjugated materials via trans-esterification reactions. The premonomers are polymerized using specific amounts of CBr_4 and are subsequently eliminated to result in the desired conjugated polymers that are analyzed by means of SEC, see Table 1. It is important to note that SEC determination of molecular weights of PPVs is not straightforward. MHKS coefficients are mostly unavailable in literature and already small differences in the PPV defect structure may have a profound effect on the hydrodynamic volume of the chains. Thus, specific MHKS parameters were determined for MDMO-PPV via analysis of several broad polymer distributions using viscometry and MALLS detection. Via usage of polymer samples with precisely known mass, dn/dc is directly obtained from the RI detector signal and MHKS values were fitted to the light scattering M_w data. For MDMO precursor polymer obtained via the sulfinyl route, $\alpha = 0.67605$ and $k = 0.000142$ mL·g^{-1} and for conjugated MDMO-PPV $\alpha = 0.809$ and $k = 0.00002$ mL·g^{-1} were obtained. Care has to be taken using MALLS detection, as the fluorescent properties of the materials lead to light emission interfering with the MALLS scatter signals. For that reason, MALLS is not easily applied and can thus not be used as a routine method for molar mass determination in this case. For the determination of MHKS values, samples were measured repeatedly at different concentrations to rule out interfering effects. For MDMO-PPV polymers obtained from the DTC route and for the CPM polymer, no specific MHKS were deduced. While parameters for the conjugated polymer should in principle be independent from the polymerization route (a concept that may be debated when going into detail), and hence MHKS for sulfinyl and DTC-made MDMO-PPV should be identical, no absolute M_n can be given for CPM-PPV. Only apparent M_n^{app} are thus given for this system.

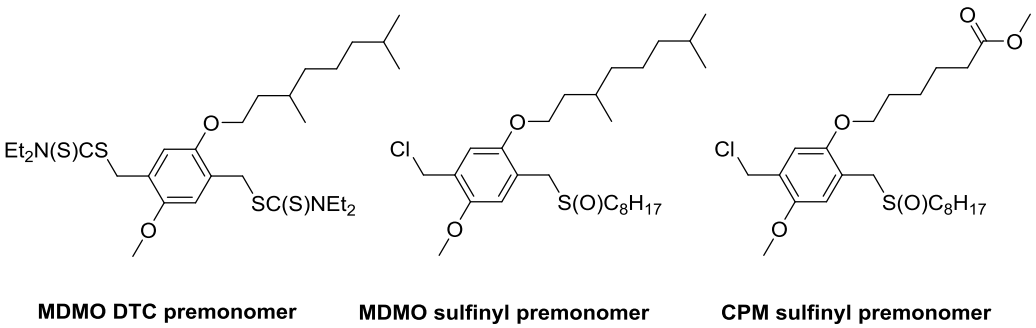

Scheme 7. Overview of the different PPV premonomers used in this study.

Table 1. Molecular weight data of conjugated MDMO-PPVs obtained from the sulfinyl (reactions at 30 °C using [*Monomer*] = 0.14 mol·L^{-1} and [*Base*] = 0.16 mol·L^{-1}) and DTC (reactions at 35 °C using [*Monomer*] = 0.20 mol·L^{-1} and [*Base*] = 0.87 mol·L^{-1}) route under variation of the amount of CBr_4.

MDMO-PPV (DTC Route)			**MDMO-PPV (Sulfinyl Route)**			**CPM-PPV (Sulfinyl Route)**		
CTA equiv.	M_n g·mol^{-1}	*Đ*	CTA equiv.	M_n g·mol^{-1}	*Đ*	CTA equiv.	M_n^{app} g·mol^{-1}	*Đ*
0	98,000	2.9	0	88,900	2.6	0	82,000	2.3
0.04	54,000	3.2	0.5	31,000	2.3	0.5	20,000	3.2
0.05	49,600	3.8	1	28,400	2.5	1	14,000	1.9
0.1	30,500	3.0	2	8,900	1.8	2	6,780	2.1
0.25	11,900	2.3	4	9,800	1.8	4	6,800	2.2
0.5	2,460	2.0	8	11,000	2.0	8	6,410	2.3
0.75	2,480	1.2	12	8,700	1.6	-	-	-
0.9	1,260	1.1	14	9,900	1.7	-	-	-
1	430	1.2	16	9,600	1.6	-	-	-
8	500	1.1	20	6,700	1.5	-	-	-
-	-	-	25	8,800	1.7	-	-	-

SEC analysis on the resulting conjugated MDMO-PPVs allows for chain transfer constant determination by fitting the inverse of the degree of polymerization as a function of the CTA to premonomer concentration ratio, following the well-known Mayo relation:

$$\frac{1}{DP_n} = \frac{1}{DP_n^o} + C_{tr}\frac{c_{CTA}}{c_M} \quad (1)$$

In this equation, DP_n represents the average degree of polymerization, DP_n^o the average degree of polymerization in an ideal case in absence of any transfer agent, C_{CTA} the transfer agent concentration and C_M the premonomer concentration. C_{tr} is the chain transfer constant and is defined as the ratio of the transfer rate coefficient k_{tr} over the propagation rate coefficient k_p. Thus, in case $k_p >> k_{tr}$ a C_{tr} smaller than unity will be obtained. In Figure 1, the Mayo plots for conjugated MDMO-PPV, polymerized via the sulfinyl and the DTC route using CBr_4 as CTA is given (see Appendix Figure A1 for the Mayo plot of CPM-PPV and Figure A2 for the corresponding SEC elugrams). Results clearly indicate the good molecular weight control over both polymerizations upon changing the control agent concentration. Nevertheless, compared to classical vinyl polymerizations, an immense amount of CBr_4 is needed to reach this effect. Whereas in vinyl polymerizations, few mole percent of CTA are sufficient to expect

good control, several equiv. of CTA are required in both precursor monomer routes. Up to 12 equiv. of control agent are needed to decrease the molecular weight of sulfinyl MDMO-PPV from 100,000 to 12,000 g·mol^{-1}. Standard MDMO-PPV polymerizations result in a yellow viscous oil for the precursor polymer and a red solid upon thermal elimination of the precursor to the conjugated polymer. Upon increasing amount of CBr_4, not only does the color of the conjugated MDMO-PPV changes from red to orange, also the physical appearance (from solid to viscous oil) changes, indicating the effect of the CTA on the chain length of the resulting MDMO-PPVs.

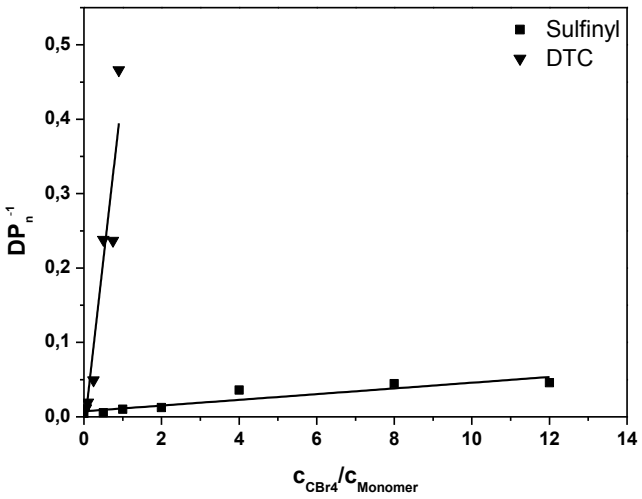

Figure 1. Inverse of the degree of polymerization as a function of the CTA to premonomer concentration ratio for MDMO-PPV synthesized via the sulfinyl and the DTC route.

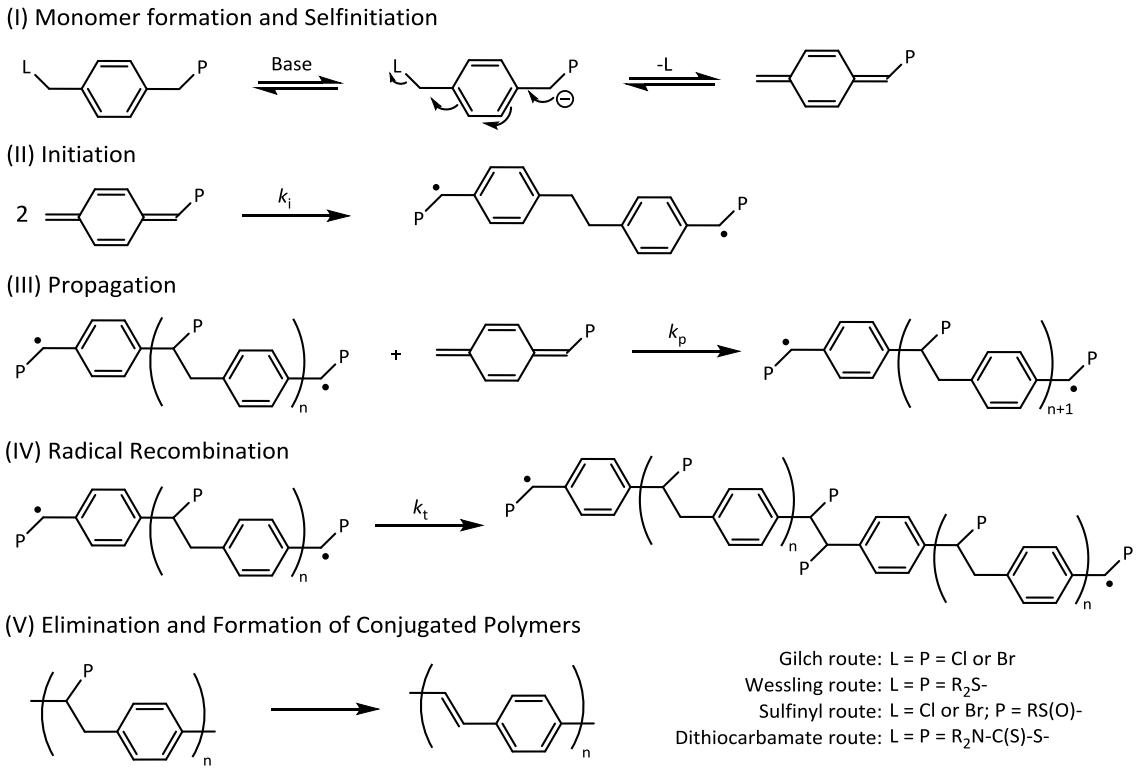

Scheme 8. Reaction mechanism of precursor polymerizations and subsequent conversion of precursor polymers to conjugated PPV.

Interestingly, a further increase in control agent concentration above 8–12 equiv.—up to 25 equiv. was tested—does not decrease the molecular weight any further. This indicates that the chain transfer agent only controls molecular weight from a certain chain length on. For sulfinyl precursor MDMO-PPV, a minimum of roughly 25 repeating monomers are added to the chain before chain termination by transfer occurs. It should be noted that the precursor polymerization is not only complicated by the fact that the polymerization is rapid, but also by the fact that initiation proceeds via a biradical formation (see Scheme 8 for full mechanism of the polymerization), hence requiring the transfer events to occur before chains are effectively dead.

Polymerizations of MDMO-PPV using the DTC precursor route show an effect of the CTA at much lower CTA concentrations. With 0.04 equiv. of CBr_4 a reduction in molecular weight is observed from 100,000 to 54,000 $g \cdot mol^{-1}$, in comparison to 10-fold higher concentrations being required in the sulfinyl route to achieve the same effect. Increasing the CBr_4 content to one equiv. reduces chain growth to such a high extent that basically no polymerization is taking place anymore. This disparate chain transfer behavior is well represented in the individual transfer constants that are determined from the data. For both polymerizations in the sulfinyl route, for $T = 30$ °C a C_{tr} of 0.0034 is obtained in good agreement with our previous study, indicating that the small change in the side chain has no or only very little kinetic effect on the polymerization [39]. For the DTC route polymerization, a C_{tr} of 0.46 at $T = 35$ °C is obtained (see Table 2), thus at a value much closer to conventional vinyl polymerization. This increased transfer constant indicates that either transfer to CBr_4 is favored in this route, or that propagation is significantly slower (or in principle a combination of the two is operational). In either way, control in the DTC route is simpler to achieve compared to the sulfinyl route and further endeavors into controlling this type of polymerization should take the DTC route into account.

Table 2. Chain transfer constant for conjugated PPVs synthesized via the sulfinyl ($T = 30$ °C) and DTC ($T = 35$ °C) precursor routes.

Conjugated PPVs	Chain Transfer Constant C_{tr}
MDMO-PPV (DTC route)	0.46
MDMO-PPV (sulfinyl route)	0.0038
CPM-PPV (sulfinyl route)	0.0034

In further investigations, a deeper look into the chain transfer kinetics of the sulfinyl route was taken. Despite the better performance of the DTC route, similarly good materials can be accessed at higher equiv. of CBr_4 in the sulfinyl route. Moreover, even though general uncertainties exist for precursor polymerizations with respect to mechanism and individual rate coefficients, the sulfinyl route is amongst the best studied precursor routes [16–20]. Further systematic kinetic investigation of this reaction type is thus highly useful and thus the reason why—in spite of the better results for the DTC route—further investigation still focuses on the sulfinyl route. To date, no reliable initiation, propagation or termination coefficients are available for any precursor polymerizations, but efforts to fill this gap have been so far mostly focused on the sulfinyl route.

A closer look towards the activation energy of chain transfer can help in understanding the otherwise rapid sulfinyl route polymerization. Polymerizations under variation of the CTA concentration were thus

conducted at different temperatures and analyzed towards the conjugated MDMO-PPV polymer (see Figure 2, Table 3 and Appendix Table A1).

Results clearly demonstrate that upon increase in reaction temperature, a decrease in the transfer constant is followed. At the same time, lower DP_n^o is reached with increasing temperature, indicating that also the ratio of termination, propagation and initiation changes strongly with temperature. The decreasing C_{tr} indicates that either propagation increases stronger with temperature than radical transfer, or that transfer becomes overall less effective at higher temperatures. Analysis of the Arrhenius relation for C_{tr} yields an apparent activation energy $E_A(C_{tr})$ of the coupled parameter of −12.8 kJ·mol^{-1} (see Figure 3). The negative value is explained by the relation $E_A(C_{tr}) = E_A(k_{tr}) - E_A(k_p)$. The negative value thus indicates that the activation energy of propagation is larger than that of transfer. Under assumption that radical transfer is usually associated with activation energies in the range of 20 kJ·mol^{-1}, the conclusion can be drawn that the activation energy of propagation is in the range of 30 kJ·mol^{-1} or higher, a value that is common for radical propagation reactions.

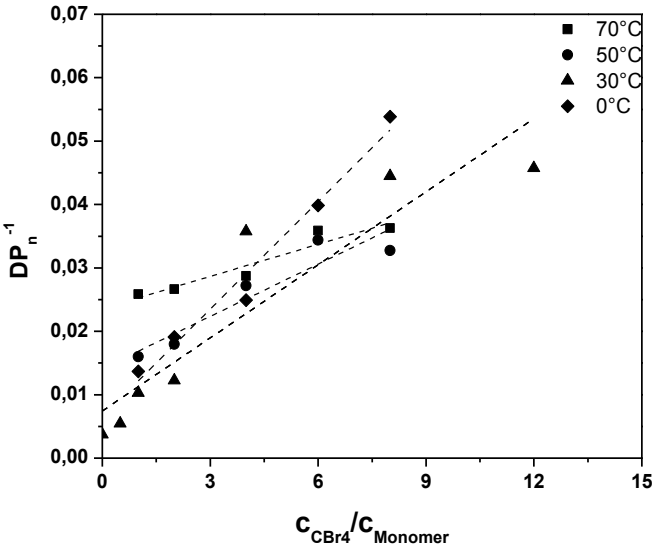

Figure 2. Inverse of the degree of polymerization as a function of the CTA to premonomer concentration ratio for MDMO-PPV synthesized via the sulfinyl "precursor" route at different polymerization temperatures.

Table 3. Chain transfer constants determined from the plots given in Figure 2 for conjugated MDMO-PPV synthesized via the sulfinyl "precursor" route at different polymerization temperatures.

T	C_{tr}
0 °C	0.0056
30 °C	0.0034
50 °C	0.0028
70 °C	0.0017

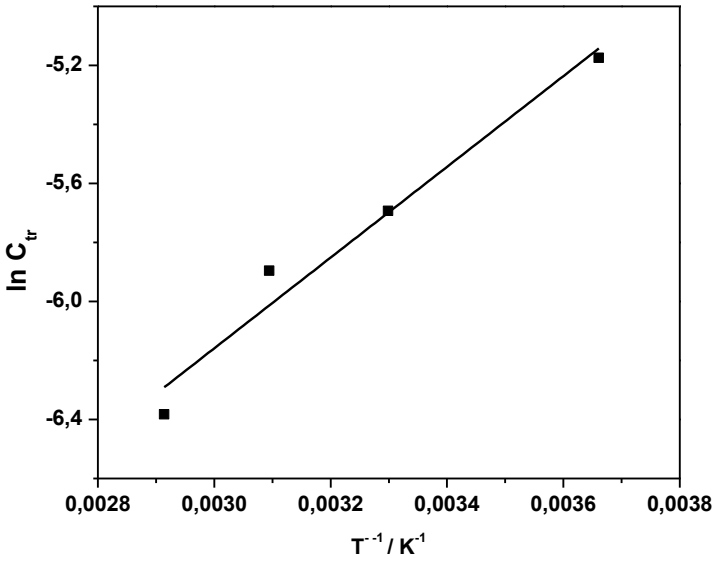

Figure 3. Arrhenius plot of C_{tr} obtained in the temperature range of 0–70 °C.

The above kinetic experiments nicely demonstrate the general difficulty to carry out controlled radical polymerizations to obtain PPV materials. The sulfinyl route is less susceptible to interfering transfer reactions, but allows for facile access of chain-length controlled polymers when several equiv. of transfer agent are employed. The dithiocarbamate route is simpler to control, which is reflected by a close to 100-fold difference in the specific chain transfer constant. Determination of the activation energy of the transfer constant for the sulfinyl route shows that less control is achieved with increasing reaction temperatures due to the high activation energy of the propagation reaction. This information may seem trivial on first glance, yet for a polymerization system for which to date only very few kinetic parameters are known, this is a significant advance in knowledge. Any additional rate parameter (or at least activation energy) that becomes available will aid in future modelling studies and a paramount understanding of the polymerization. Only with such models at hand, rational selection of reaction conditions will be possible and true product control achieved.

3.2. Chain Extension via Sequential Approaches Using MDMO-PPV Macro Initiators

While the above experiments demonstrate the ability to control molecular weight, not much is yet known about the endgroup distribution in the polymer products. In principle, by the halogen transfer of the CTA, a bromine-end-functional polymer should be obtained with high endgroup fidelity. Such groups are in principle suitable to be used in post-polymerization modifications either in endgroup exchange reactions or in subsequent controlled polymerizations. More precisely, the bromine chain end can be used as a macroinitiator moiety for copper-mediated radical polymerization chain extensions with vinylic monomers, or can be replaced by an azide to give access to CuAAC conjugation reactions. In both ways, block copolymers can be synthesized. As a detailed kinetic investigation on the sulfinyl route was performed in the first part, also block copolymer formation via this route are taken into account. Post-polymerization reactions concerning the DTC route will be presented in a forthcoming study.

3.2.1. Block Copolymer Formation Using ATRP Conditions

In a first approach, atom transfer radical polymerizations (ATRP) are performed on bromine end-capped sulfinyl MDMO precursor PPV to generate block copolymers in a sequential approach, in accordance to the first experiments that we have shown before [39]. MDMO-PPVs (precursor level) with bromine end groups were synthesized using the sulfinyl precursor route and 8 equiv. of CBr_4 as chain transfer agent, resulting in polymers with a molecular weight of 6900 $g \cdot mol^{-1}$. The CTA needs to be thoroughly removed using preparative recycling GPC, since it can by itself act as initiator in an ATRP process. The precursor MDMO-PPV-Br polymer was then used for block copolymerizations. It has to be noted that chain extension is only possible on precursor polymer level (thus before elimination of the sulfinyl groups). Otherwise, interactions between the conjugated chain system and Cu(I)Br can lead to undesired oxidation reactions on one hand and defects in the polymer structure on the other hand. Reactivation of the bromine end group via ATRP reactions are carried out at 75 °C, using BuOAc as solvent and Cu(I)Br and Me_6TREN as salt/ligand system. In a first step, chain extensions with *t*BuA are executed. The influence of both the reaction time as well as monomer concentration is investigated. Reactions are stopped by precipitation of the polymer followed by removal of the copper on a short alumina column. Since elimination of precursor PPV starts at 75 °C, all precursor block copolymers are in a second step thermally eliminated (3 h at 110 °C) and purified, resulting in true conjugated MDMO-PPV-*b*-P*t*BuA block copolymers. SEC analysis is always performed on the final conjugated block copolymers in order to allow for a meaningful comparison between different samples (the hydrodynamic volume of the PPVs change significantly from precursor to conjugated polymer, thus making comparisons of molecular weights between both states difficult).

Figure 4 depicts the molecular weight distributions of conjugated MDMO-PPV and the chain extended MDMO-PPV-*b*-P*t*BuA block copolymers, obtained during chain extension with 100 equiv. of *t*BuA relative to the precursor polymer after purification. A clear shift towards higher molecular weights upon increasing reaction times (and hence acrylate conversion) is observed. A full shift of the distributions is thereby indicative that almost all PPV chains have been reinitiated and that bromine-endgroup fidelity was good. Dispersity shows a slight increase, which may be indicative of slow reinitiation. Furthermore, changes in the concentration of acrylate (50 and 100 equiv., see Table 4) show a good correlation between apparent M_n^{app} (note that only apparent values are discussed since SEC determination was carried out via polystyrene calibration) and starting monomer concentration. With a constant reaction time of 4 h, a doubling in the (apparent) block length of the polyacrylate is seen upon doubling the amount of monomer. ATR FT-IR analysis (See Appendix Figure A3) also supports the successful chain extension via ATRP reaction conditions after purification of the resulting mixture by precipitation in an ice-cold MeOH/H_2O (1/1) solution and filtration of the block copolymer. After chain extension, both the characteristic PPV peaks as well as the acrylate-typical carbonyl peaks are clearly detectable. Previous UV-Vis measurements on PPV block copolymer formation via both the anionic [35] as well as radical [39] route showed a slight influence of the non-conjugated block on the λ_{max} values of the conjugated system, by detecting a small blue shift in the spectra. Similar shifts are expected for the current block copolymers synthesized in here and no additional measurements were performed as the practical consequences with regards to fluorescence are overall expected to be small.

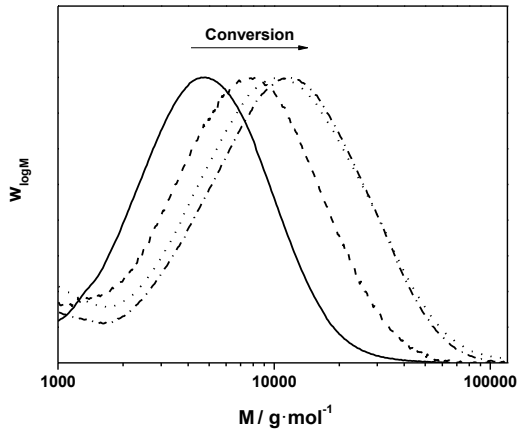

Figure 4. Molecular weight distributions of MDMO-PPV (black line) and MDMO-PPV-*b*-P*t*BuA block copolymers obtained from ATRP with 100 equiv. of monomer followed in time (dotted lines with increasing conversion from left to right).

Table 4. Apparent average molecular weights of MDMO-PPV-*b*-P*t*BuA block copolymers from ATRP chain extensions using different equiv. of monomer.

MDMO-PPV homopolymer and block copolymers	M_n^{app} g·mol^{-1}	M_w^{app} g·mol^{-1}	$Đ$
MDMO-PPV	6,900	9,970	1.40
MDMO-PPV-*b*-P*t*BuA 50 equiv. *t*BuA	8,200	12,900	1.60
MDMO-PPV-*b*-P*t*BuA 100 equiv. *t*BuA	9,200	16,600	1.80

The above observations are mostly qualitative, thus additional quantitative investigations into the ATRP chain extension were also undertaken. ATRPs were conducted with both *t*BuA and styrene and monomer conversion was followed gravimetrically. If reactions were well controlled, not only shifts in the molecular weight as indicated above should be expected, but also first order kinetics for monomer consumption (to test for constant radical concentration). For both styrene and the acrylate, linear first order plots are observed with only small deviations from the linear behavior in the initial time regime, see Figure 5. The acrylate polymerizes in the first 30 min of the polymerization significantly faster than styrene and only after that period, similar reaction rates are observed for the following reaction.

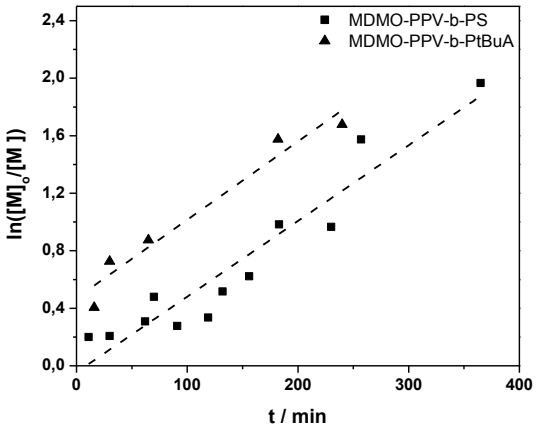

Figure 5. Semi-logarithmic first order kinetic plot of MDMO-PPV-*b*-P*t*BuA and MDMO-PPV-*b*-PS block copolymerizations via ATRP.

Figure 6 depicts for the same polymerizations the evolution of number-average molecular weight as a function of conversion, nicely demonstrating the good correlation of experimental with theoretical molecular weights. Note that the different offsets of M_n in Figure 6 stem from different PPV precursor polymers being used in the reactions. Thus, it may be concluded that the combination of the radical CBr_4 sulfinyl precursor PPV route and ATRP chain extension technique allows for the synthesis of a variety of PPV containing block copolymers of different sizes, functionalities and properties in an easy fashion.

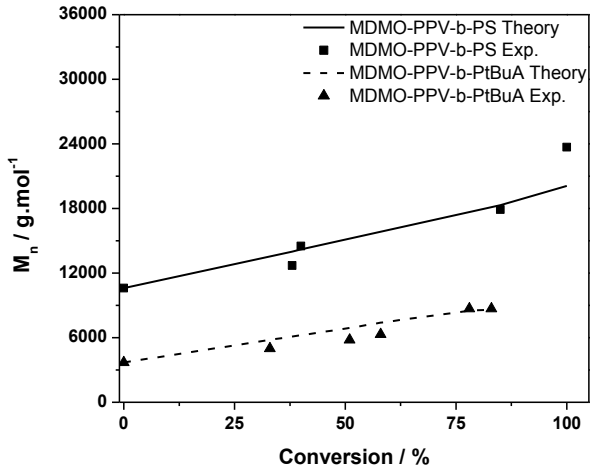

Figure 6. The dependence of the molecular weight M_n upon the conversion for the MDMO-PPV-*b*-PtBuA and MDMO-PPV-*b*-PS block copolymers. Markers represent experimental M_n values, the lines theoretical M_n.

3.2.2. Block Copolymer Formation Using SET-LRP Conditions

An alternative route to chain extend bromine endcapped precursor PPV is to make use of single electron transfer-living radical polymerization (SET-LRP) [45]. With SET-LRP, chain extension can be carried out at room temperature in a polar reaction medium, disabling any premature elimination of the PPV precursor units in the resulting block copolymer that could interfere with the polymerization. The drawback is that most PPV systems (such as MDMO-PPV) are too apolar to effectively be dissolved in the polar solvents used in the SET-LRP reaction. Therefore, the more polar precursor CPM-PPV was used in the following to test the chain extension via SET-LRP. The ester moiety of the CPM side chain allows for good solubility in DMF and successful chain extensions with *t*BuA and MA could be carried out at room temperature (see Table 5 and Appendix Figure A4). SET-LRP reaction conditions (DMF as solvent, a reaction temperature of 25 °C and reaction time of 4 h) in combination with 100 equiv. of monomer indicate an increase in M_n of the precursor CPM-PPV from 7300 to 11,400 g·mol^{-1} or 11,800 g·mol^{-1} for *t*-BuA or methyl acrylate (MA), respectively. In a subsequent step, all block copolymers were eliminated again, to enable correct comparison of the different techniques (ATRP and SET-LRP). Styrene was tested as monomer in SET-LRP reactions as well; however, no shift in molecular weight was observed.

Table 5. Apparent average molecular weights of block copolymers obtained from SET-LRP of CPM-PPV employing 100 equiv. of monomer and a reaction temperature of 25 °C.

Monomer	Precursor Polymer			Conjugated Polymer		
	M_n^{app} g·mol^{-1}	M_w^{app} g·mol^{-1}	*Đ*	M_n^{app} g·mol^{-1}	M_w^{app} g·mol^{-1}	*Đ*
-	7,300	15,600	2.10	8,900	19,200	2.10
***t*-BuA**	11,400	24,200	2.10	12,600	26,600	2.10
MA	11,800	32,200	2.70	13,400	24,600	1.80

3.3. Conjugation of PPV Block Copolymers Using CuAAC Conditions

Sequential approaches towards successful block copolymerization (e.g., ATRP or SET-LRP) restrict the choice of the second block to vinyl-type monomers that are able to undergo (controlled) radical polymerization. Thus, the development of a modular approach allowing any combination of building blocks is also highly attractive. Therefore, copper-catalyzed alkyne-azide cycloaddition (CuAAC) is employed for the synthesis of PPV block copolymers. As a first attempt, MDMO-PPV-*b*-PEG block copolymers were targeted using such a modular approach. Therefore, bromine endcapped precursor sulfinyl MDMO-PPV was first functionalized at elevated temperatures with an azide group, using an excess amount of sodium azide (10 equiv. to polymer) in DMF. In a second step, the obtained precursor MDMO-PPV-azide is then clicked to a PEG-alkyne using standard CuAAC reaction conditions. Reactions are carried out at 25 °C, using DMF as solvent and Cu(I)Br and PMDETA as catalyst. Both precursors PPV and PEG were added in equimolar amounts to avoid excesses of homopolymer being left after reaction. The reaction mixture was allowed to stir for an extended time (up to three days) after which copper was removed from the product mixture by passing the solution over a short alumina column. In a second step, all precursor block copolymers are eliminated, resulting in conjugated MDMO-PPV-*b*-PEG block copolymer. Results regarding molecular weight and dispersity for the starting MDMO-PPV homopolymer and the resulting MDMDO-PPV-*b*-PEG block copolymer can be found in Table 6 and molecular weight profiles are plotted in Figure 7.

As can be seen from the molecular weight distributions in Figure 7, a bimodal SEC profile is obtained after reaction, representing a mixture of two separate distributions—MDMO-PPV homopolymer—and the block copolymer MDMO-PPV-*b*-PEG, indicating a partly successful ligation. Comparison of the starting materials *Mp* indicated that the click reaction by itself was successful, but that pure PPV remained—whether due to reaction inefficiencies or due to insufficient functionalization of the homopolymer. Closer inspection and repetitions of the CuAAC reaction leads to the conclusion that the partial success (no improvement is seen even after three days' reaction time under varying conditions) is due to solubility issues. As mentioned before, the azide functionalized MDMO-PPV does not dissolve well in DMF, which can make the azide partially inaccessible for reaction. Purification of the MDMO-PPV-b-PEG block copolymer from the homopolymer leftovers is far from trivial. Residual PEG can relatively easily be removed by washing the mixture with water, residual MDMO-PPV can only be removed by preparative recycling SEC, as was done before [44].

Table 6. Molecular weights and *Đ* for the homopolymers and conjugated MDMO-PPV-*b*-PEG block copolymer.

MDMO-PPV homo- and di-block copolymer	M_n^{app} g·mol^{-1}	M_w^{app} g·mol^{-1}	M_p^{app} g·mol^{-1}	*Đ*
MDMO-PPV-N_3	7,800	12,400	8,300	1.60
PEG-alkyne	6,400	6,600	7,300	1.10
MDMO-PPV-*b*-PEG	-	-	18,400	-

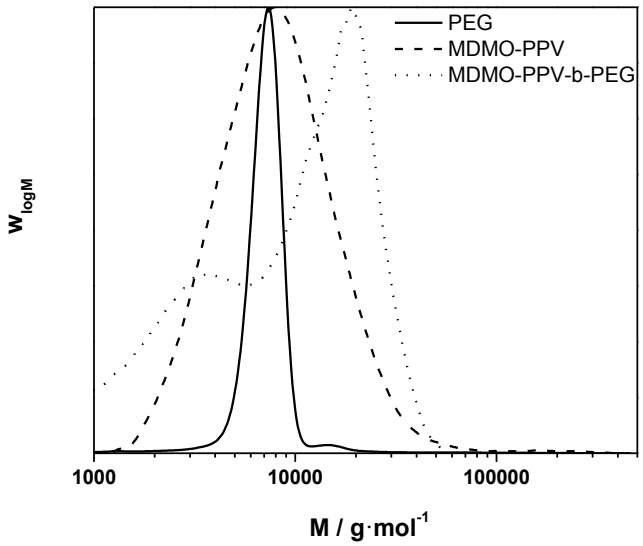

Figure 7. SEC profile for the direct coupling of alkyne-functionalized PEG to azide functionalized eliminated MDMO-PPV using click conditions without purification of the homopolymer leftovers.

As solubility of the polymers may play a significant role in the somewhat hindered click reaction, synthesis of triblock copolymers from successive chain transfer polymerization, ATRP chain extension with an acrylate and CuAAC conjugation was tested, yielding material with the desired structure MDMO-PPV-*b*-P*t*BuA-*b*-PEG. MDMO-PPV-*b*-P*t*BuA-Br polymers as discussed above were modified with NaN_3 to obtain azide-functional material. The generally better solubility of the acrylate block and the higher chain flexibility of the second block should aid in the click reaction and improve the system. Furthermore, P*t*BuA can at a later stage be eliminated to yield poly(acrylic acid) blocks and thus give access to pH-responsive triblock copolymer structures. The CuAAC reaction with PEG-alkyne was then again allowed to react for three days under the same conditions of the diblock CuAAC conjugation reaction, after which the reaction is stopped by precipitation of the resulting triblock copolymers in ice-cold hexane followed by removal of the copper on a short alumina column. After thermal elimination of the material and precipitation, an orange colored conjugated MDMO-PPV-*b*-P*t*BuA-*b*-PEG was obtained. Molecular weight distributions of the individual homo-, di- and resulting tri-block copolymers as well as corresponding molecular weights are presented in Table 7 and Figure 8. The CuAAC conjugation shows in this case good success.

Table 7. Average molecular weights and *Đ* for the MDMO-PPV-*b*-P*t*BuA-*b*-PEG triblock copolymers and its precursors.

MDMO-PPV di- and tri-block copolymers	M_n^{app} g·mol^{-1}	M_w^{app} g·mol^{-1}	M_p^{app} g·mol^{-1}	*Đ*
MDMO-PPV	6,100	9,300	8,060	1.50
MDMO-PPV-*b*-P*t*BuA	7,300	11,800	10,500	1.60
PEG-alkyne	6,400	6,600	6,500	1.10
MDMO-PPV-*b*-P*t*BuA-*b*-PEG	-	-	19,200	-

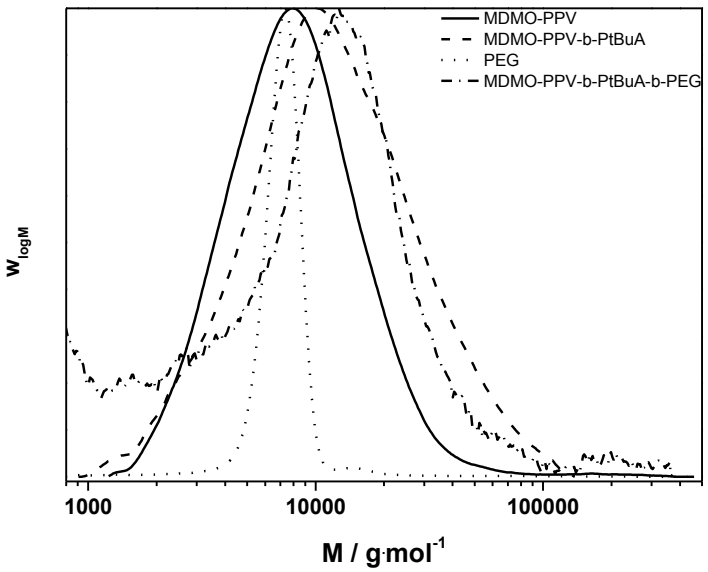

Figure 8. Molecular weight distributions of the clicked MDMO-PPV-*b*-P*t*BuA-*b*-PEG triblock copolymer and its precursors.

The ATRP chain extension yields similar good results as in the case described above. The CuAAC reaction proceeds well. The triblock copolymer product distribution still shows some material at the lower molecular weight side of the distribution, which could not be removed by precipitation or washing. Thus, no average molecular weights could be determined and again only M_p is discussed. The MDMO-PPV-*b*-P*t*BuA copolymer has a peak molecular weight of 10,500 g·mol^{-1}. The PEG-alkyne block has a molecular weight of 6500 g·mol^{-1}. In the sum, the triblock structure features a M_p of 19,200 g·mol^{-1}, which can be regarded as a good match—taking into account that no calibration exists for these materials and large variations in the MHKS parameters of the chains must be expected with each consecutive chain extension.

4. Conclusions

The concept of controlling the precursor polymerization of PPV via the use of a CBr_4 chain transfer agent has been studied in detail. Control over molecular weight is achieved by using several equiv. of CTA compared to precursor monomer. Systematic kinetic investigations confirmed that better chain length control is achieved when polymerizations are carried out at lower temperatures. Via determination of the activation energy of the coupled parameter C_{tr} (−12.8 kJ·mol^{-1}), important information on the propagation reaction could be gathered, which will aid in future modelling studies that aim at the final elucidation of the to-date only partially understood PPV polymerization mechanism. Interestingly, easier

control is achieved in the precursor polymerization, when the dithiocarbamate polymerization route is employed compared to the sulfinyl route, hinting at large differences in radical stability and propagation tendency between the two types of monomers.

PPVs with number average molecular weights between 10,000 and 100,000 $g \cdot mol^{-1}$ are obtained by varying the amount of CTA, allowing large scale synthesis of these polymers in a wide range of molecular weights. In addition to good control over chain length, high chain-end fidelity could be demonstrated. Employment of the PPV-Br species that are obtained from the chain transfer polymerization as macroinitiators in copper-mediated radical polymerizations allowed for the facile synthesis of several diblock copolymer structures, either via the ATRP or the SET-LRP route. For SET-LRP, better results were obtained when PPVs with more polar side groups, such as in CPM-PPV, were used. Concomitantly, also the *click*-type conjugation of PPV was investigated. Direct substitution of the terminal bromine at the PPV chain end followed by CuAAC conjugation with an alkyne-functionalized PEG yielded only partial success. Significant improvement of the CuAAC was seen when the PPVs were first chain extended with *t*-butyl acrylate to make the terminal bromine/azide functionality more accessible. In this way, MDMO-PPV-*b*-P*t*BuA-*b*-PEG was obtained successfully, giving rise to high precision multiblock organic semiconductor materials.

The CTA-based synthesis procedure thus allows for relatively easy—and most importantly—scalable synthesis of well-controlled PPV materials, a task that is otherwise very hard to achieve. Chain length control and especially the ability to form more complex macromolecular structures in both sequential and modular design approaches allows to build in PPV segments into virtually any existing polymer architecture. This advancement in field opens a variety of possibilities for PPVs outside the classical application domain of organic electronics. Investigations into the application of such materials for bioimaging or biosensing are currently underway in our laboratories.

Appendix Information

A1. Synthetic Procedures

1.1. 1-(Chloromethyl)-5-((3,7-dimethyloctyl)oxy)-2-methoxy-4-((octylsulfinyl)methyl)benzene (MDMO) Sulfinyl Premonomer

1.1.1. 3,7-Dimethyloctyl-4-methylbenzene sulfonate (**2**) [46]

A mixture of **1** (115.7 g, 0.732 mol, 1 equiv.) and *p*-toluenesulfonyl chloride (143 g, 0.732 mol, 1 equiv.) in CH_2Cl_2 (500 mL) was cooled with a mixture of $CHCl_3$ and liquid nitrogen while KOH (166 g, 2.981 mol, 4 equiv.) was added under nitrogen atmosphere. After addition of the base—enabling temperatures below 5°C—the reaction was stirred for 3 h at 0 °C. The reaction was quenched with ice water (500 mL), extracted with CH_2Cl_2 (3 × 250 mL) and the organic layer was dried over anhydrous $MgSO_4$. After filtration, evaporation of the solvent under reduced pressure gave the crude product **2** as a clear oil, Scheme S1. No purification was needed (214.80 g, 93.9%). ^{1}H-NMR ($CDCl_3$): δ = 7.74 (m, 2H); 7.30 (m, 2H); 4.01 (m, 2H); 2.39 (s, 3H); 1.59 (m, 1H); 1.42 (m, 3H); 1.06 (m, 6H); 0.79 (m, 9H).

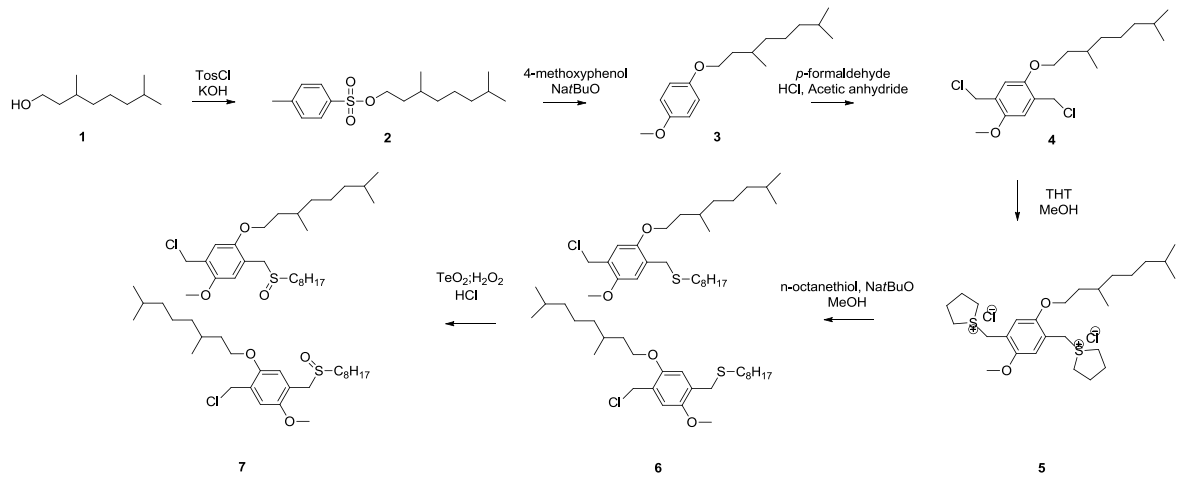

Scheme A1. Synthesis route for MDMO premonomer via the sulfinyl precursor route.

1.1.2. 1-((3,7-Dimethyloctyl)oxy)-4-methoxy benzene (**3**)

4-methoxyphenol (75.45 g, 0.608 mol, 1 equiv.) and NaO*t*Bu (70.49 g, 0.735 mol, 1.21 equiv.) in EtOH (600 mL) was stirred for 1 h at room temperature under nitrogen atmosphere. **2** (208.9 g, 0.67mol, 1.1 equiv.) was added and the complete mixture was stirred overnight at reflux temperature (80 °C). The reaction was quenched with H_2O (600 mL), extracted with CH_2Cl_2 (3 × 250 mL) and the organic layer was dried over anhydrous $MgSO_4$. After filtration, evaporation of the solvent under reduced pressure gave the crude product as a brown oil. The pure product **3** was obtained by vacuum distillation at 95 °C, Scheme S1. (120.36 g, 75.1%). ^{1}H-NMR ($CDCl_3$): δ = 6.83 (s, 4H); 3.92 (s, 2H); 3.76 (s, 3H); 1.78 (s, 1H); 1.56 (m, 3H); 1.31 (s, 4H); 1.17 (s, 2H); 0.89 (s, 9H). ^{13}C-NMR ($CDCl_3$): δ = 154.1 (C4); 152.6 (C4); 115.8 (CH); 115.6 (CH); 67.2 (CH_2); 55.8 (CH_3); 39.2 (CH_2); 37,6 (CH_2); 37,1 (CH_2); 29.2 (CH_2); 28.7 (CH_2); 23.2 (CH_3); 15.24 (CH_3). DIP MS (CI, *m*/*z*): 265 (M+), 220/221 (M^+−OEt), 142/143 (M^+−OPhOMe). FT−IR (ATR): ν = 2995, 2482, 1516, 825, 749 cm^{-1}.

1.1.3. 2,5-Bis(chloro-methyl)-1-(3,7-dimethyloctyloxy)-4-methoxybenzene (**4**)

To a stirred mixture of **3** (120.63 g, 0.46 mol, 1 equiv.) and *p*-formaldehyde (37.76 g, 1.25 mol, 2.75 equiv.), HCl (37%, 296.60 g, 3.01 mol, 6.6 equiv.) was added drop wise at room temperature under nitrogen atmosphere. Subsequently acetic anhydride (466 g, 4.56 mol, 10 equiv.) was added drop wise, without exceeding a temperature of 70 °C. The solution was stirred at 70 °C for 4 h. After cooling down to room temperature, H_2O (600 mL) was added to the solution. The resulting precipitate was filtered off and redissolved in CH_2Cl_2 (400 mL). Next, the organic solution was dried over anhydrous $MgSO_4$ and filtered. Evaporation of the solvent under reduced pressure gave the crude product as a yellow oil. The pure product **4** was obtained by recrystallization in hexane as white crystals, Scheme S1. (102.3 g, 61.43%). M_p: 65 °C. ^{1}H-NMR ($CDCl_3$): δ = 6.90 (s, 4H); 4.61 (s, 4H); 4.00 (s, 2H); 3.84 (s, 3H); 1.80 (s, 2H); 1.61 (m, 5H); 1.29 (m, 2H); 1.12 (m, 2H); 0.90 (m 9H); ^{13}C-NMR ($CDCl_3$): δ = 19.8 (CH_3); 22.6 (CH_3); 24.6 (CH_2); 27.9 (CH), 30.2 (CH_2), 36.6 (CH_2), 37.4 (CH_2), 39.2 (CH_2), 41.2 (CH_2), 56.4 (CH_3), 67.9 (CH_2), 113.2 (C4), 114.3 (C4), 127.0 (C4). DIP MS (CI, *m*/*z*): 361 (M+), 326 (M^+−Cl), 290 (M^+−2Cl); FT−IR (ATR): ν = 2948, 2878, 1977, 1508, 1459, 1401, 885, 881, 735, 690 cm^{-1}.

1.1.4. 1,4-Bis(tetrahydrothiopheniomethyl)xylene dichloride (**5**)

To a stirred mixture of **4** (65.94 g, 0.18 mol, 1 equiv.) in MeOH (600 mL), tetrahydrothiophene (THT) (80.45 g, 0.91 mol, 5 equiv.) was added. The reaction was allowed to react at room temperature for 3 days. The solution was precipitated in cold acetone (2 L) under heavy stirring and the resulting precipitate was filtered off and washed with cold acetone. After drying under vacuum, the pure product **5** was obtained as a white solid, Scheme S1 (60.78 g, 60.04%). M_p: 81–83 °C. ^{1}H-NMR (D_2O): δ = 7.10 (s, 2H); 4.41 (s, 4H); 4.08 (m, 4H); 3.80 (s 2H); 3.40 (d, *J* = 5.5 Hz, 8H); 2.22 (m, 8H); 1.74 (m, 2H); 1.55–1.37 (m, 3H); 1.18 (m, 6H); 0.84 (d, *J* = 6.3 Hz, 3H); 0.71 (dd, *J* = 6.6 and 2.9, 6H). ^{13}C-NMR (D_2O): δ = 19.10, (CH_3); 22.07 (CH_3); 24.13 (CH_2); 26.4 (CH); 29.6 (CH); 30.7 (CH_2); 31.3 (CH_2); 37.6 (CH_2); 38.7 (CH_2); 40.9 (CH_2); 43.9 (CH_2); 45.5 (CH_2); 58.6 (CH_3); 70.0 (CH_2); 117.8/118.6 (CH); 121.9/122.4 (C4); 153.7/154.3 (C4). DIP MS (CI, *m*/*z*): 556 (MH^+), 524 (M^+–Cl), 432 (M^+–THT–Cl), 296 (M^+-2 THT–Cl–CH_2). FT–IR (ATR): ν = 3016, 2926, 2462, 1633, 1514, 1463, 1417, 1317, 1226, 920, 786, 699 cm^{-1}.

1.1.5. (4-(Chloromethyl)-2-((3,7-dimethyloctyl)oxy)-5-methoxybenzyl)(octyl)sulfane (**6**)

A mixture of *n*-octanethiol (15.82 g, 0.108 mol, 1 equiv.) and NaO*t*Bu (10.04 g, 0.108 mol, 1 equiv.) in MeOH (240 mL) was stirred at room temperature for 30 min. This mixture was added drop wise to a stirred mixture of **5** (60.0 g, 0.108 mol, 1 equiv.) in MeOH (360 mL) after which it was allowed to react for 3 h at room temperature under nitrogen atmosphere. After evaporation of the solvent under reduced pressure, *n*-octane (100 mL) was added and evaporated again to remove the THT by azeotropic distillation. This procedure was repeated 5 times. The residue was redissolved in CH_2Cl_2 (350 mL), extracted with a saturated NaCl:H_2O solution (1:10) (3 × 250 mL) and the organic layer was dried over anhydrous $MgSO_4$. After filtration, evaporation of the solvent under reduced pressure gave the crude product **6** as a white solid (49.03 g, 96.9%), which was used without further purification, Scheme S1. ^{1}H-NMR ($CDCl_3$): δ = 6.87 (m, 2H); 4.62 (d, *J* = 2.4 Hz, 2H); 3.99 (m, 2H); 3.84 (m, 3H); 3.70 (d, *J* = 3.4 Hz, 2H); 2.45 (t, *J* = 6.8 Hz, 2H); 1.87 (m, 1H); 1.81 (m, 1H); 1.52 (m, 2H); 1.25 (m, 18H); 0.88 (m, 9H).

1.1.6. 1-(Chloromethyl)-5-((3,7-dimethyloctyl)oxy)-2-methoxy-4-((octylsulfinyl)methyl)benzene (**7**)

To a stirred mixture of **6** (49.0 g, 0.104 mol, 1 equiv.) in 1,4-dioxane (800 mL), TeO_2 (2.075 g, 0.013 mol, 0.125 equiv.) and HCl (2 M, 4.9 mL, 0.122 mol, 1.2 equiv.) were added. To start the reaction H_2O_2 (35%, 20.20 g, 0.208 mol, 2 equiv.) was added and the reaction was followed on TLC (hexane/EtOAc: 6/4). As soon as all **6** was consumed, the reaction was quenched with a saturated NaCl-solution:H_2O (1:1; 400 mL). The solution was extracted with CH_2Cl_2 (3 × 300 mL), dried over anhydrous $MgSO_4$ and filtered. Evaporation of the solvent under reduced pressure gave the crude product as a yellow oil. The pure product **7** was obtained by column chromatography (SiO_2, hexane/EtOAc: 6/4), Scheme S1 (25.48 g, 50.36%). M_p: 109.5–110.5 °C. ^{1}H-NMR ($CDCl_3$): δ = 7.37 (d, *J* = 8.0 Hz, 2H); 7.26 (d, *J* = 8.0 Hz, 2H); 4.55 (s, 2H); 3.91 + 3.93 (dd, J_{AB} = 13.0 Hz, 2H); 2.53 (t, *J* = 8.0 Hz, 2H); 1.70 (m, 2H); 1.36 (m, 2H); 1.23 (m, 8H); 0.84 (t, *J* = 6.8 Hz, 3H); ^{13}C NMR ($CDCl_3$,100 MHz): δ = 14.0 (CH_2); 22.4 (CH_3); 22.5 (CH_3); 28.7 (CH); 28.9 (CH_2); 29.1 (CH);

31.6 (CH_2); 45.6 (CH_2), 51.0 (CH_2); 57.6 (CH_3); 129.1 (C4); 130.2 (C4); 130.3 (C4); 137.5 (C4). DIP MS (CI, *m*/*z*): 488 (MH^+), 451/453 (M^+–Cl), 325/327 (M^+–S(O)C_8H_{17}), 291 (M^+–Cl–S(O)C_8H_{17}), 174 (S(O)C_8H_{17}); FT–IR (ATR): ν = 2959, 2918, 2847, 1520, 1457, 1405,919, 754, 689 cm^{-1}.

1.2. 6-(5-Chloromethyl-4-methoxy-2-octylsulfinylmethylphenoxy)-Hexanoic Acid Methyl Ester (CPM) Sulfinyl Premonomer

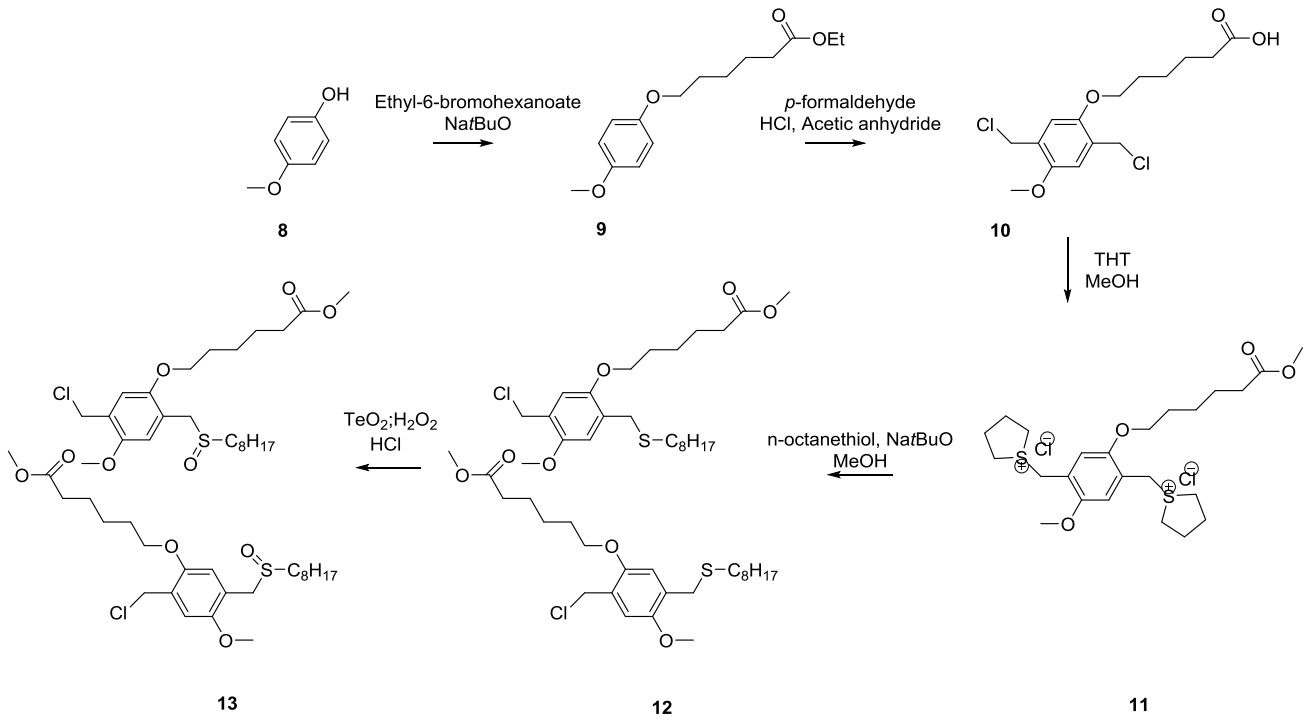

Scheme A2. Synthesis route for CPM premonomer via the sulfinyl precursor route.

1.2.1. 6-(4-Methoxy-phenoxy)-hexanoic acid ethyl ester (**9**)

A mixture of **8** (93.5 g, 0.75 mol, 1 equiv.) and NaO*t*Bu (86.6 g, 0.90 mol, 1.2 equiv.) in EtOH (500 mL) was stirred for 1 h at room temperature under nitrogen atmosphere. A solution of ethyl-6-bromohexanoate (200 g, 0.90 mol, 1.2 equiv.) and NaI (3.4 g, 0.02 mol, 1.2 equiv.) in EtOH (200 mL) was added and the complete mixture was stirred for 4 h at reflux temperature (80 °C). The reaction was quenched with H_2O (400 mL), extracted with CH_2Cl_2 (3 × 100 mL) and the organic layer was dried over anhydrous $MgSO_4$. After filtration, evaporation of the solvent under reduced pressure gave the crude product as an orange oil. The pure product **9** was obtained by recrystallization in MeOH as white crystals. Scheme S2 (131.61 g, 65.70%). M_p: 30 °C. ^{1}H-NMR ($CDCl_3$): δ = 6.80 (s, 4H); 4.10 (q, *J* = 7.3 Hz, 2H); 3.88 (t, *J* = 6.4 Hz, 2H); 3.74 (s, 3H); 2.30 (t, *J* = 7.6 Hz, 2H); 1.74 (m, 2H); 1.68 (m, 2H); 1.47 (m, 2H); 1.23 (t, *J* = 7.2 Hz, 3H). ^{13}C-NMR ($CDCl_3$): δ = 173.74 (C4); 153.65 (C4); 153.13 (C4); 115.35 (CH); 114.56 (CH); 68.24 (CH_2); 60.24 (CH_2); 55.70 (CH_3); 34.25 (CH_2); 29.04 (CH_2); 25.65 (CH_2); 24.72 (CH_2); 14.24(CH_3). DIP MS (CI, *m*/*z*): 266 (M+), 221/222 (M^+–OEt), 143/144 (M^+–OPhOMe), 124/125 (M^+–C_5H_{10}COOEt). FT–IR (ATR): ν = 2938, 2479, 2000, 1866, 1732, 1506, 1476, 1292, 1233, 1160, 1112, 1033, 825, 742 cm^{-1}.

1.2.2. 6-(2,5-Bis-chloromethyl-4-methoxy-phenoxy)hexanoic acid (**10**)

To a stirred mixture of **9** (131.6 g, 0.49 mol, 1 equiv.) and *p*-formaldehyde (40.9 g, 1.35 mol, 2.75 equiv.), HCl (37%, 110.1 g, 3.26 mol, 6.6 equiv.) was added drop wise at 0 °C under nitrogen atmosphere. Subsequently acetic anhydride (503 g, 4.94 mol, 10 equiv.) was added drop wise, without exceeding a temperature of 70 °C. The solution was stirred at 60 °C for 3 h. After cooling down to room temperature, H_2O (400 mL) was added to the solution. The resulting precipitate was filtered off and redissolved in CH_2Cl_2 (200 mL). Next, the organic solution was dried over anhydrous $MgSO_4$ and filtered. Evaporation of the solvent under reduced pressure gave the crude product as a yellow oil. The pure product **10** was obtained by recrystallization in EtOAc as white crystals, Scheme S2 (71.7 g, 41.74%). M_p: 99 °C. ^{1}H-NMR ($CDCl_3$): δ = 6.90 (d, *J* = 3.9 Hz, 2H); 4.60 (d, *J* = 3.5 Hz, 4H); 3.98 (t, *J* = 6.2 Hz, 2H); 3.83 (s, 3H); 2.39 (t, *J* = 7.4 Hz, 2H); 1.82 (m, 2H); 1.72 (m, 2H); 1.56 (m, 2H). ^{13}C-NMR ($CDCl_3$): δ =171.95 (C4); 151.65 (C4); 151.13 (C4); 127.67 (C4); 127.41 (C4); 114.98 (CH); 113.90 (CH); 69.24 (CH_2); 61.06 (CH_2); 58.80 (CH_3); 41.93 (CH_2); 41.85 (CH_2); 34.53 (CH_2); 29.54 (CH_2); 26.14 (CH_2); 24.93 (CH_2); 21.62 (CH_2); 14.75 (CH_3). DIP MS (CI, *m*/*z*): 334 (M+), 299 (M^+–Cl), 263 (M^+–2Cl), 220/222 (M^+–$C_5H_{10}COOH$). FT–IR (ATR): ν = 2938, 2875, 1971, 1724, 1687, 1512, 1463, 1410, 1312, 1220, 1141, 1033, 875, 871, 732, 686 cm^{-1}.

1.2.3. 6-(2,5-Bis-chloroemthyl-4-methoxy-phenoxy) hexanoic acid methyl ester (**11**)

To a stirred mixture of **10** (71.7 g, 0.22mol, 1 equiv.) in MeOH (600 mL), tetrahydrothiophene (THT) (99.8 g, 1.1 mol, 5 equiv.) was added. The reaction was allowed to react at 50 °C for 4 days. The solution was precipitated in cold diethyl ether (1 L) under heavy stirring and the resulting precipitate was filtered off and washed with cold diethyl ether. After drying under vacuum, the pure product **11** was obtained as a white solid, Scheme S2 (40.0 g; 33.85%). M_p: 119 °C. ^{1}H-NMR (D_2O): δ = 7.08 (s, 1H); 7.06 (s, 1H); 4.41 (s, 2H); 4.40 (s, 2H); 4.01 (t, *J* = 6.3 Hz, 2H); 3.79 (s, 3H); 3.56 (s, 3H); 3.40 (m, 8H); 2.32 (t, *J* = 6.3 Hz, 2H); 2.24 (m, 8H); 1.75 (m, 2H); 1.59 (m, 4H); 1.42 (m, 2H). ^{13}C-NMR ($CDCl_3$): δ = 179.43 (C4); 178.03 (C4); 152.56 (C4); 152.54 (C4); 151.89 (C4); 151.86 (C4); 120.40 (CH); 120.33 (CH); 116.78 (CH); 116.03 (CH); 69.78 (CH_2); 56.94 (CH_3); 52.75 (CH_3); 49.53 (CH_2); 45.47 (CH_2); 43.83 (CH_2); 43.77 (CH_2); 42.18 (CH_2); 34.34 (CH_2); 34.20 (CH_2); 29.08 (CH_2); 28.70 (CH_2); 25.64 (CH_2); 24.69 (CH_2). DIP MS (CI, *m*/*z*): 525 (MH^+), 493 (M^+–Cl), 401 (M^+–THT–Cl), 265 (M^+–2 THT–Cl–CH_2). FT–IR (ATR): ν = 3004, 2942, 2879, 2122, 1732, 1510, 1449, 1399, 1313, 1225, 1033, 909, 773, 702 cm^{-1}.

1.2.4. 6-(5-Chloromethyl-4-methoxy-2-octylsulfanylmethyl-phenoxy)hexanoic acid methyl ester (**12**) [47]

A mixture of *n*-octanethiol (12.31 g, 83.9 mmol, 1.1 equiv.) and NaO*t*Bu (8.1 g, 76.3 mmol, 1 equiv.) in MeOH (300 mL) was stirred at room temperature for 30 min. This mixture was added drop wise to a stirred mixture of **11** (40.0 g, 76.3 mmol, 1 equiv.) in MeOH (700 mL) after which it was allowed to react for 2 h at room temperature under N_2 atmosphere. After evaporation of the solvent under reduced pressure, *n*-octane (100 mL) was added and evaporated again to remove the THT. This procedure was repeated 5 times. The residue was redissolved in CH_2Cl_2 (350 mL), extracted with a saturated NaCl-solution:H_2O (1:10) (3 × 250 mL) and the organic layer was dried over anhydrous $MgSO_4$.

After filtration, evaporation of the solvent under reduced pressure gave the crude product **12** as a white solid (26.0 g, 67.5%) and used without further purification, Scheme S2. ^{1}H-NMR ($CDCl_3$): δ = 6.85 (m, 2H); 4.61 (s, 1H); 4.60 (s, 1H); 3.94 (m, 2H); 3.80 (m, 3H); 3.69 (d, *J* = 3.5 Hz, 2H); 3.65 (s, 3H); 2.45 (t, *J* = 6.8 Hz, 2H); 2.33 (t, *J* = 7.4 Hz, 2H); 1.79 (m, 2H); 1.65 (m, 2H); 1.52 (m, 2H); 1.24 (m, 12 H); 0.85 (m, 3H).

1.2.5. 6-(5-Chloromethyl-4-methoxy-2-octylsulfinylmethyl-phenoxy)-hexanoic acid methyl ester (**13**)

To a stirred mixture of **12** (26.0 g, 56.6 mmol, 1 equiv.) in 1,4-dioxane (350 mL), TeO_2 (1.1 g, 7.1 mmol, 1/8 equiv.) and HCl (1 M, 10 mL, 1.2 equiv.) were added. To start the reaction H_2O_2 (35%; 11.01 g 113.3 mmol, 2 equiv.) was added and the reaction was followed on TLC (hexane/ EtOAc; 5/5). As soon as all **12** was consumed, the reaction was quenched with a saturated Na_2SO_3-solution:H_2O (1:1; 400 mL). The solution was extracted with CH_2Cl_2 (3 × 300 mL), dried over anhydrous $MgSO_4$ and filtered. Evaporation of the solvent under reduced pressure gave the crude product as a yellow oil. The pure product **13** was obtained by column chromatography (SiO_2, hexane/EtOAc 5/5)(45.97 mmol, 21.80 g, 81.22%), Scheme S2. M_p: 35 °C. ^{1}H-NMR ($CDCl_3$): δ = 6.76 (s, 1H); 6.75 (s, 1H); 4.44 (s, 2H); 3.63 (d, *J* = 7 Hz, 4H); 3.48 (s, 3H); 3.47 (s, 3H); 2.45 (t, *J* = 7.4 Hz, 2H); 2.15 (t, *J* = 7.4 Hz, 2H); 1.65–1.45 (m, 6H); 1.32–1.05 (m, 12H); 0.69 (t, *J* = 6.6 Hz, 3H). ^{13}C-NMR ($CDCl_3$): δ = 174.55 (C4); 174.42 (C4); 151.79 (C4); 151.54 (C4); 127.18 (C4); 120.43 (C4); 115.23 (CH); 113.44 (CH); 69.17 (CH_2); 56.74 (CH_3); 53.48 (CH_2); 52.03 (CH_2); 51.90 (CH_3); 41.93 (CH_2); 41.85 (CH_2); 34.34 (CH_2); 32.25 (CH_2); 29.54 (CH_2); 29.39 (CH_2); 26.16 (CH_2); 23.13 (CH_2); 14.61 (CH_3). DIP MS (CI, *m*/*z*): 475/477 (MH^+), 439/441 (M^+–Cl), 313/315 (M^+–S(O)C_8H_{17}), 279 (M^+–Cl–S(O)C_8H_{17}), 162/163 (S(O)C_8H_{17}). FT–IR (ATR): ν = 3003, 2942, 2881, 2409, 1732, 1545, 1510, 1447, 1400, 1313, 1220, 1165, 1104, 1034, 909, 774, 686 cm^{-1}.

1.3. 2,5-Bis(N,N-diethyldithiocarbamate-methyl)-1-(3,7-dimethyloctyloxy)-4-methoxybenzene (MDMO) DTC Premonomer

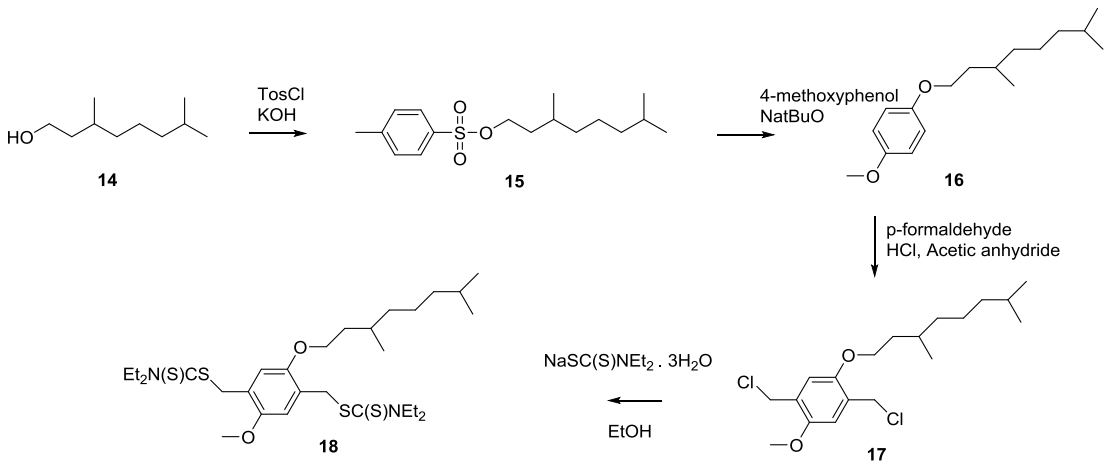

Scheme A3. Synthesis route for MDMO premonomer via the dithiocarbamate route.

Synthesis of 2,5-bis(chloro-methyl)-1-(3,7-dimethyloctyloxy)-4-methoxy benzene (**17**) was similar to synthesis of product **4**. All properties were in agreement with the previously reported materials.

1.3.1. 2,5-Bis(N,N-diethyldithiocarbamate-methyl)-1-(3,7-dimethyloctyloxy)-4-methoxybenzene (**18**).

To 50 mL of an ethanol solution of **17** (1 g, 2.767 mmol, 1 equiv.), sodium diethyldithiocarbamate trihydrate (1.445 g, 6.365 mmol, 2.3 equiv.) was added as a solid. The mixture was stirred for 3 h at room temperature under a nitrogen atmosphere. Subsequently, 50 mL of water was added and the mixture was filtered over a Buchner to obtain white crystals which were washed with ethanol and water and used without further purification, Scheme S3. Yield: 100%; M_p: 70.2−70.7 °C; ^{1}H-NMR ($CDCl_3$): δ = 6.99 (s, 2H); 4.52 (s, 2H); 4.48 (s, 2H); 3.95 (m, 4H+2H); 3.74 (s, 3H); 3.64 (m, 4H); 1.60–1.85 (m, 2H); 1.38–1.58 (m, 2H); 1.21 (t, 12H); 1.05–1.30 (m, 6H); 0.88 (d, 3H); 0.81 (d, 6H). ^{13}C NMR ($CDCl_3$): δ = 196.11 (CH); 195.99 (CH); 151.27 (C4); 150.90 (C4); 125.08 (CH); 124.42 (CH); 114.75 (CH); 113.86 (CH); 67.13 (CH_2); 56.19 (CH_3); 49.41 (CH_2); 49.34 (CH_2); 46.61 (CH_2); 39.22 (CH_2); 37.32 (CH_2); 36.83 (CH_2); 36.30 (CH_2); 29.79 (CH_2); 27.95 (CH_2); 24.69 (CH_3); 22.69 (CH_2); 22.59 (CH_2); 19.62 (CH_2); 12.42 (CH_3); 11.59 (CH_3). DIP-MS (EI, *m*/*e*): 148 (M^+ SC(S) NEt_2), 116 (C(S)NEt_2); FT–IR (NaCl): ν = 2954, 2930, 2869, 1485, 1415, 1268, 1207 cm^{-1}.

A2. SEC Results of Conjugated MDMO-PPV Using CBr_4 as CTA

Table A1. Overview of SEC results of conjugated MDMO-PPV using different equiv. of CBr_4 at varying reaction temperatures.

Reaction Temp. °C	CTA equiv.	M_n^{app} g·mol^{-1}	M_w^{app} g·mol^{-1}	*Đ*
0	1	39,200	87,300	2.20
	2	26,400	57,500	2.10
	4	19,400	36,600	1.90
	6	12,200	20,400	1.70
	8	9,300	13,900	1.50
30	0	77,500	272,600	3.50
	0.5	53,100	106,100	2.00
	1	56,000	134,500	2.40
	2	36,100	92,300	2.60
	4	12,800	34,300	2.70
	8	7,700	23,200	3.00
	12	7,600	15,300	2.00
	14	9,900	15,400	1.90
	16	10,600	14,800	1.60
	20	6,700	15,200	1.50
	25	8,800	10,400	1.80
50	1	31,300	75,700	2.40
	2	27,000	53,500	2.00
	4	18,200	40,500	2.20
	6	14,200	20,400	1.40
	8	14,900	24,800	1.70
70	1	23,200	51,000	2.20
	2	22,700	43,000	1.90
	4	17,800	32,000	1.80
	6	13,400	21,800	1.60
	8	13,900	22,500	1.60

A3. Mayo Plot and Elugrams CPM Sulfinyl Premonomer

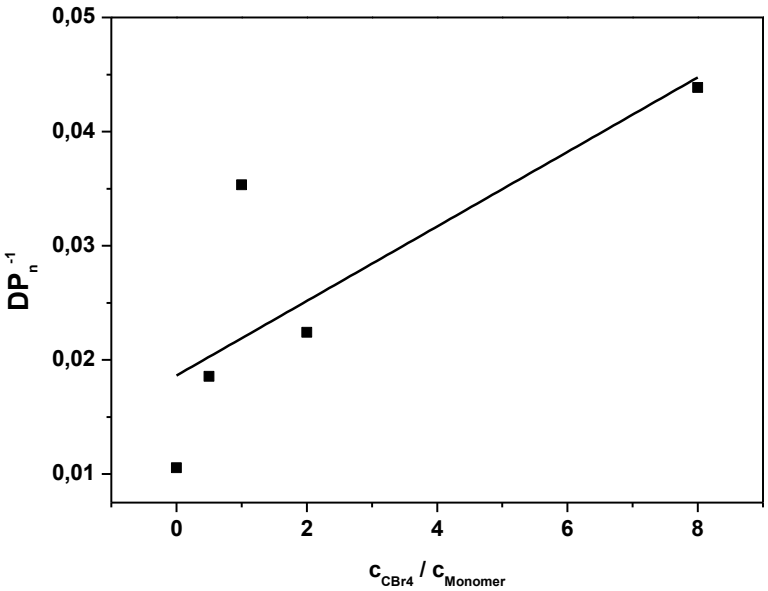

Figure A1. Inverse of the degree of polymerization as a function of the CTA to monomer concentration ratio for CPM-PPV synthesized via the sulfinyl precursor route.

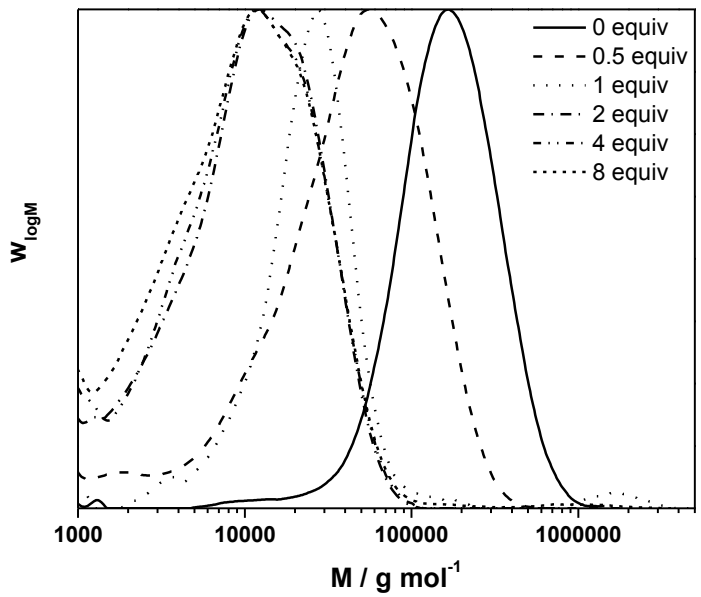

Figure A2. SEC profile of CPM-PPV obtained by polymerization of the sulfinyl CPM premonomer in the presence of specified amounts of CBr_4 as CTA, followed by elimination of the precursor polymer into conjugated CPM-PPV.

A4. ATR FT-IR Results of MDMO-PPV-*b*-P*t*BuA

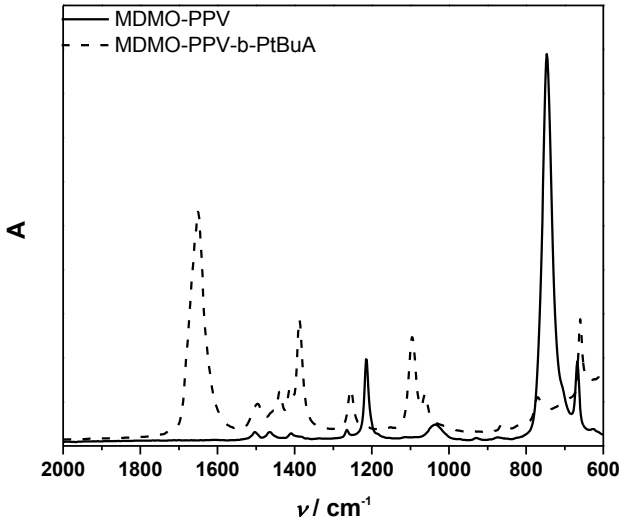

Figure A3. ATR FT-IR spectra for MDMO-PPV and MDMO-PPV-*b*-P*t*BuA.

A5. SEC Results CPM-PPV Block Copolymer Formation

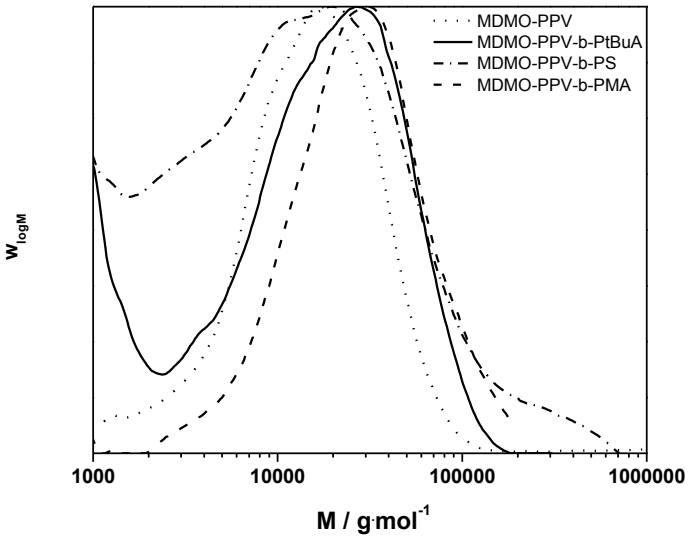

Figure A4. GPC profile of bromine functionalized MDMO-PPV and MDMO-PPV-*b*-P*t*BuA, MDMO-PPV-*b*-PS, MDMO-PPV-*b*-PMA block copolymers using SET-LRP reaction conditions.

Acknowledgments

Neomy Zaquen is grateful for the funding from the "Agency for Innovation by Science and Technology" in Flanders (IWT), Joke Vandenbergh and Thomas Junkers are grateful for funding from the "Fund for Scientific Research". In Flanders (FWO) in the framework of the Odysseus scheme and for the FWO postdoctoral fellowship grant of Joke Vandenbergh. This research has been funded by the Interuniversity Attraction Poles Programm (P7/05) initiated by the Belgium Science Policy Office.

Author Contributions

Neomy Zaquen performed most of the CTA experimental work as well as all work on (tri)block copolymer synthesis, Joke Vandenbergh performed part of the work on the CTA experiments as well as supervision of the research, Maria Schneider deduced MHKS parameters for the polymers and Laurence Lutsen, Dirk Vanderzande and Thomas Junkers directed and supervised the research.

Conflicts of Interest

The authors declare no conflict of interest.

References

1. Günes, S.; Neugebauer, H.; Sariciftci, N.S. Conjugated polymer-based organic solar cells. *Chem. Rev*. **2007**, *107*, 1324–1338.
2. Kulkarni, A.P.; Tonzola, C.J.; Babel, A.; Jenekhe, S.A. Electron transport materials for organic light-emitting diodes. *Chem. Mater*. **2004**, *16*, 4556–4573.
3. Gomez, E.D.; Lee, S.S.; Kim, C.S.; Loo, Y.-L. Morphological Control of Solution-Processed Thin Films in Organic Electronics. In *Molecular Organic Electronics Devices*. Nova Science Publishers: Hauppauge, New York, NY, USA, 2010; Chapter 4, pp. 109–152.
4. Horowitz, G. Organic field-effect transistors. *Adv. Matter* **1998**, *10*, 365–377.
5. Cooreman, P.; Thoelen, R.; Manca, J.; VandeVen, M.; Vermeeren, V.; Michiels, L.; Ameloot, M.; Wagner, P. Impedimetric immunosensors based on the conjugated polymer PPV. *Biosens. Bioelectron*. **2005**, *20*, 2151–2156.
6. Matharu, Z.; Arya, S.K.; Singh, S.P.; Gupta, V.; Malhotra, B.C. Langmuir–Blodgett film based on MEH-PPV for cholesterol biosensor. *Anal. Chim. Acta* **2009**, *634*, 243–249.
7. Junkers, T.; Vandenbergh, J.; Adriaensens, P.; Lutsen, L.; Vanderzande, D. Synthesis of poly(*p*-phenylene vinylene) materials via the precursor routes. *Polym. Chem*. **2012**, *3*, 275–285.
8. Odian, G. *Principles of Polymerization*, 4th ed.; Wiley–Interscience: Hoboken, NJ, USA, 2004; Chapter 3.
9. Karpagam, S.; Guhanathan, S.; Sakthivel, P. Applications of wittig reactions in dibenzo 18-crown−6−ether substituted phenylenevinylene oligomer—synthesis, photo luminescent, and dielectric properties. *J. Appl. Polym. Sci*. **2011**, *120*, 960–967.
10. Wessling, R.A.; Zimmerman, R.G. Polyelectrolytes from bis sulfonium salts. US Patent 3401152, 10 September 1968.
11. Gilch, H.G.; Weelwright, W.L. Polymerization of α-halogenated *p*-xylenes with base. *J. Polym. Sci. Polym. Chem. Ed*. **1966**, *4*, 1337–1349.
12. Wessling, R.A.; Zimmerman, R.G. Polyxylylidene articles. US Patent 3706677, 23 February 1972.
13. Denton, F.R.; Serker, A.; Lathi, P.M.; Garay, R.O.; Karasz, F.E. Para-Xylylenes and analogues by base-induced elimination from 1,4-bis-(dialkylsulfoniomethyl)arene salts in poly(1,4-arylene vinylene) synthesis by the wessling soluble precursor method. *J. Polym. Sci. A Polym. Chem*. **1992**, *30*, 2233–2240.

14. Son, S.; Dodabalapur, A.; Lovinger, A.J.; Galvin, M.E. Luminescence enhancement by the introduction of disorder into poly(*p*-phenylene vinylene). *Science* **1995**, *269*, 376–378.
15. Kesters, E.; Gilissen, S.; Motmans, F.; Lutsen, L.; Vanderzande, D. Polymerization behaviour of xanthate-containing monomers toward PPV precursor polymers: Study of the elimination behavior of precursor polymers and oligomers with *in situ* FT-IR and UV−Vis analytical techniques. *Macromolecules* **2002**, *35*, 7902–7910.
16. Louwet, F.; Vanderzande, D.; Gelan, J.; Mullens, J. A new synthetic route to a soluble high molecular weight precursor for poly(*p*-phenylenevinylene) derivatives. *Macromolecules* **1995**, *28*, 1330–1331.
17. Louwet, F.; Vanderzande, D.; Gelan, J. A general synthetic route to high molecular weight poly(*p*-xylylene)-derivatives: a new route to poly(*p*-phenylene vinylene). *Synth. Met*. **1995**, *69*, 509–510.
18. Issaris, A.; Vanderzande, D.; Adriaensens, P.; Gelan, J. Polymerization mechanism of 1-[(butylsulfi(o)nyl)methyl]-4-(halomethyl)benzene: The effect of polarizer and leaving group. *Macromolecules* **1998**, *31*, 4426–4431.
19. Van Breemen, A.; Vanderzande, D.; Adriaensens, P.; Gelan, J. Highly selective route for producing unsymmetrically substituted monomers toward synthesis of conjugated polymers derived from poly(*p*-phenylene vinylene). *J. Org. Chem*. **1999**, *64*, 3106–3112.
20. Lutsen, L.; Van Breemen, A.; Kreuder, W.; Vanderzande, D.; Gelan, J. Highly selective route to unsymmetrically substituted 1-{2-[(butylsulfanyl)methyl]-5-(chloromethyl)-4-methoxyphenoxy}-3,7-dimethyloctane and isomers toward synthesis of conjugated polymer oc1c10 used in LEDs: Synthesis and optimization. *Helv. Chem. Acta* **2000**, *83*, 3113–3121.
21. Van Der Borght, M.; Vanderzande, D.; Adriaensens, P.; Gelan, J. Scope and limitations of a new highly selective synthesis of unsymmetrical monomers for the synthesis of precursors toward poly(arylenevinylene)s. *J. Org. Chem*. **2000**, *65*, 284–289.
22. Wessling, R.A. The polymerization of xylylene bisdialkyl sulfonium salts. *J. Polym. Sci. Polym. Symp*. **1985**, *72*, 55–66.
23. Van Breemen, A.; Issaris, A.; de Kok, M.; van Der Borght, M.; Adriaensesn, P.; Gelan, J.; Vanderzande, D. Optimization of the polymerization process of sulfinyl precursor polymers toward poly(*p*-phenylenevinylene). *Macromolecules* **1999**, *32*, 5728–5735.
24. Issaris, A.; Vanderzande, D.; Gelan, J. Polymerization of a *p*-quinodimethane derivative to a precursor of poly(*p*-phenylene vinylene)—Indications for a free radical mechanism. *Polymer* **1997**, *38*, 2571–2574.
25. Hontis, L.; Vrindts, V.; Lutsen, L.; Vanderzande, D.; Gelan, J. The gilch polymerisation towards OC1C10-PPV: Indications for a radical mechanism. *Polymer* **2001**, *42*, 5793–5796.
26. Hontis, L.; Vrindts, V.; Vanderzande, D.; Lutsen, L. Verification of radical and anionic polymerization mechanisms in the sulfinyl and the gilch route. *Macromolecules* **2003**, *36*, 3035–3044.
27. Wiesecke, J.; Rehanh, M. [2.2]Paracyclophanes with defined substitution pattern—Key compounds for the mechanistic understanding of the gilch reaction to poly(*p*-phenylene vinylene)s. *Angew. Chem. Int. Ed*. **2003**, *42*, 567–570.

28. Henckens, A.; Duyssens, I.; Lutsen, L.; Vanderzande, D.; Cleij, T. Synthesis of poly(*p*-phenylene vinylene) and derivatives via a new precursor route, the dithiocarbamate route. *Polymer* **2006**, *47*, 123–131.
29. Henckens, A.; Lutsen, L.; Vanderzande, D.; Knipper, M.; Manca, J.; Arnouts, T.; Poortman, J. In Synthesis of PTV vis the dithiocarbamate route: A new precursor route toward conjugated polymers, Proceedings of the SPIE, Organic Optoelectronics and Photonics, Strasbourg, France; 28–30 April 2004; pp. 52–59.
30. Hontis, L.; van Der Borght, M.; Vanderzande, D.; Gelan, J. Radical as well as anionic polymerisation mechanisms in the synthesis of poly(*p*-arylene vinylene) precursors. *Polymer* **1999**, *40*, 6615–6617.
31. Issaris, A.; Gelan, J.; Vanderzande, D. Study of the mechanism of the polymerisation of α-leaving group-α'-polariser-*p*-xylene Indications for a free radical mechanism. *Synth. Met*. **1997**, *85*, 1149–1150.
32. Barner-Kowollik, C.; Du Prez, F.E.; Espeel, P.; Hawker, C.J.; Junkers, T.; Schlaad, H.; van Camp, W. "Clicking" polymers or just efficient linking: What is the difference? *Angew. Chem. Int. Ed*. **2011**, *50*, 60–62.
33. Hoyle, C.E.; Bowman, C.N. Thiol–Ene click chemistry. *Angew. Chem. Int. Ed*. **2010**, *49*, 1504–1573.
34. Kolb, H.C.; Finn, M.G.; Sharpless, K.B. Click chemistry: Diverse chemical function from a few good reactions. *Angew. Chem. Int. Ed*. **2001**, *40*, 2004–2021.
35. Cosemans, I.; Vandenbergh, J.; Lutsen, L.; Vanderzande, D.; Junkers, T. Synthesis of well-defined PPV containing block copolymers with precise endgroup control from a dual-initiator strategy. *Polym. Chem.* **2013**, *4*, 3471–3479.
36. Odian, G. *Principles of Polymerization*, 3rd ed.; John Wiley & Sons, Inc.: Hoboken, NY, USA, 1991; p. 243.
37. Issaris, A. PPV-precursoren en hun polymerisatiemechanisme anionisch of toch radicalair? Ph.D. Thesis, Limburgs Universitair Centrum, Hasselt and Diepenbeek, Belgium, 1997.
38. Hontis, L. The polymerisation behaviour of *p*-quinodimethane systems: Verification of radical and anionic mechanisms in the sulfinyl and the Gilch route. Ph.D. Thesis, Limburgs Universitair Centrum, Hasselt and Diepenbeek, Belgium, 2002.
39. Vandenbergh, J.; Cosemans, I.; Lutsen, L.; Vanderzande, D.; Junkers, T. Controlled synthesis of MDMO-PPV and block copolymers made thereof. *Polym. Chem*. **2012**, *3*, 1722–1725.
40. Wang, J.S.; Matyjaszewski, K. Controlled/"living" radical polymerization. Atom transfer radical polymerization in the presence of transition-metal complexes. *J. Am. Chem. Soc*. **1995**, *117*, 5614–5615.
41. Matyjaszewski, K.; Xia, J. Atom transfer radical polymerization. *Chem. Rev.* **2001**, *101*, 2921–2990.
42. Lee, M.; Cho, B.-K.; Zin, W.-C. Supramolecular structures from rod−coil block copolymers. *Chem. Rev*. **2001**, *101*, 3869–3892.
43. De Cuendias, A.; Hiorns, R.C.; Cloutet, E.; Vignau, L.; Cramail, H. Conjugated rod–coil block copolymers and optoelectronic applications. *Polym. Int*. **2010**, *59*, 1452–1476.
44. Cosemans, I.; Vandenbergh, J.; Voet, V.S.D.; Loos, K.; Lutsen, L.; Vanderzande, D.; Junkers, T. Anionic PPV polymerization from the sulfinyl precursor route: block copolymer formation from sequential addition of monomers. *Polymer* **2013**, *54*, 1298–1304.

45. Rosen, B.M.; Percec, V. Single-electron transfer and single-electron transfer degenerative chain transfer living radical polymerization. *Chem. Rev*. **2009**, *109*, 5069–5119.
46. Becker, H.; Spreitzer, H.; Ibrom, K.; Kneuder, W. New insights into the microstructure of GILCH polymerized PPVs. *Macromolecules* **1999**, *32*, 4925–4932.
47. Van Severen, I. Design, synthesis and evaluation of functionalized poly(*p*-phenylene vinylene) derivatives: From existing structures to novel materials. Ph.D. thesis, Universiteit Hasselt, Hasselt and Diepenbeek, Belgium, 2006.